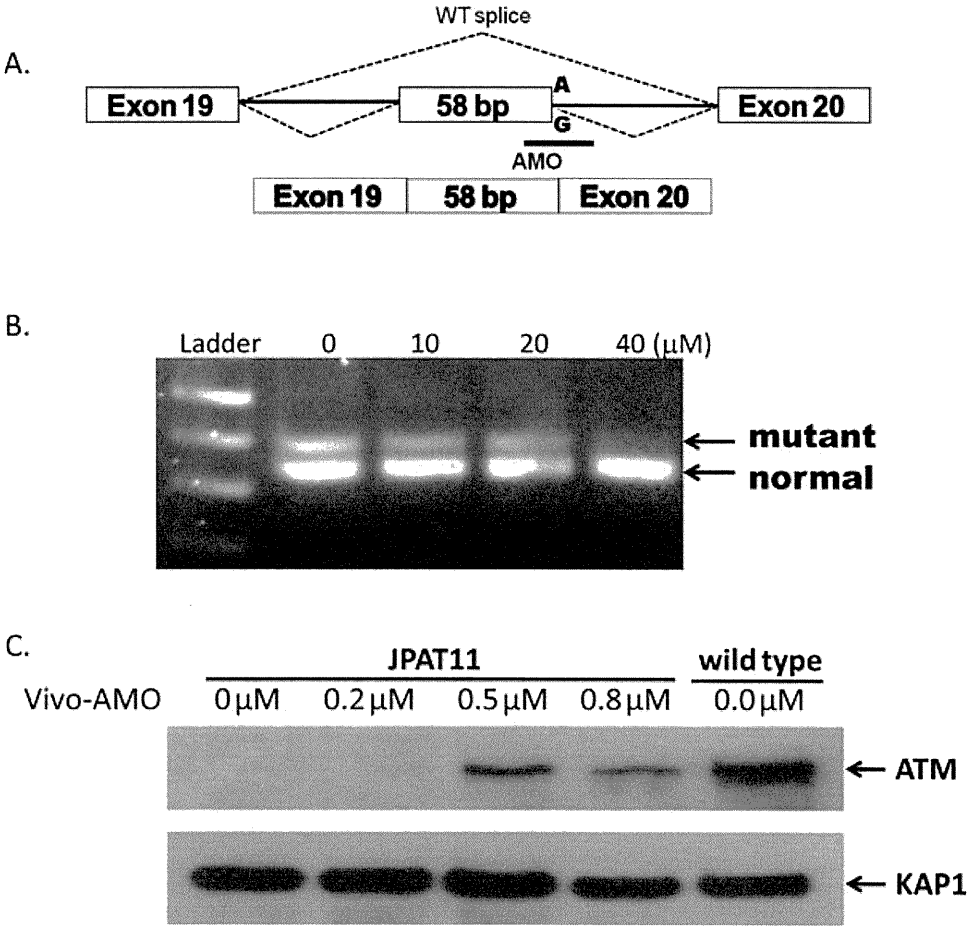

Figure 5. Correction of a splicing mutation in JPAT11 using AMO-J11. **(A)** Schematic representation of inclusion of pseudoexon (type II) and location of designed AMO. **(B)** JPAT11 cells were treated with 0, 10, 20, and 40 μM AMO for 4 days and RNAs were isolated and analyzed for corrected splicing products. **(C)** JPAT11 cells were treated with 0.2, 0.5, and 0.8 μM of Vivo-AMO-J11 for 4 days and nuclear lysates were isolated for western blotting. KAP1 antibody was used as a loading control.

days, and measured ATM autophosphorylation after DNA damage induced by IR. An aminoglycoside RTC, G418, served as a positive control. Both G418 and RTC13 successfully induced ATMpS1981 autophosphorylation as shown by (A) FC-ATMpSer1981 and (B) IRIF ATMpSer1981 assays (Fig. 6), thereby demonstrating a potential therapeutic approach for these siblings, despite the presence of a nonsense mutation in only one allele.

Discussion

Whereas a high (0.5%) coefficient of inbreeding had been recorded for the Japanese population [Pattison, 2004], the *ATM* mutation spectrum identified in our JPAT patient cohort included almost no homozygous mutations and no founder mutations. The c.4776+2T>A and c.7883_7887del5 mutations reported by Ejima and Sasaki [1998] and Fukao et al. [1998] were not observed. In fact, all mutations detected in the JPAT families—four frameshift, two nonsense, four LGDs, and six affecting splicing—were new except for a previously identified c.748C>T splicing mutation in an Irish–American family [Teraoka et al., 1999] and the c.2639-384A>G mutation [Sobeck, 2001]. It is noteworthy that only three of the six splicing mutations involved canonical sites (c.331+5G>A, c.2639-19_2639-7del13, c.8585-1G>C). In the other mutations: (1) c.748C>T (exon 9) and 4956GC>TT (exon 35) presented as nonsense mutations in gDNA, but at the cDNA level caused skipping of the exon in which they were located; and (2) JPAT11/12 had a deep-intronic mutation (c.2639-384A>G) in intron 19 that seemed to activate a cryptic acceptor splice site resulting in the insertion of a 58-bp pseudoexon in the transcript (Figs. 1, 2C, and 5).

Nonsense mutations frequently alter the splicing of the exon containing them, an observation that has been termed nonsense-associated altered splicing (NAS) [Valentine, 1998]. In most cases of NAS, the mutation disrupts an ESE critical for exon inclusion [Liu et al., 2001]. AMOs usually act by covering/masking a mutated site in the pre-mRNA, but cannot be used to correct splicing mutations at canonical sites. Thus, AMOs are most effective in correcting type II and IV splice mutations [Eng et al., 2004]. Most relevant here, AMOs can be applied to the functional analysis of *ATM* mutations. By using AMOs designed to bind the wild-type exon 9 and exon 35 sequences located around the mutation sites, we were able to induce alternative splicing (Fig. 2G and H). These results suggest that unknown regulatory elements are probably located near or at the sites of the mutation and are necessary for modulating normal splicing events in these exons. Furthermore, as described earlier, the deep-intronic mutation (c.2639-384A>G) in intron 19 is among the most attractive candidates for AMO therapy (Fig. 5) [Du et al., 2007].

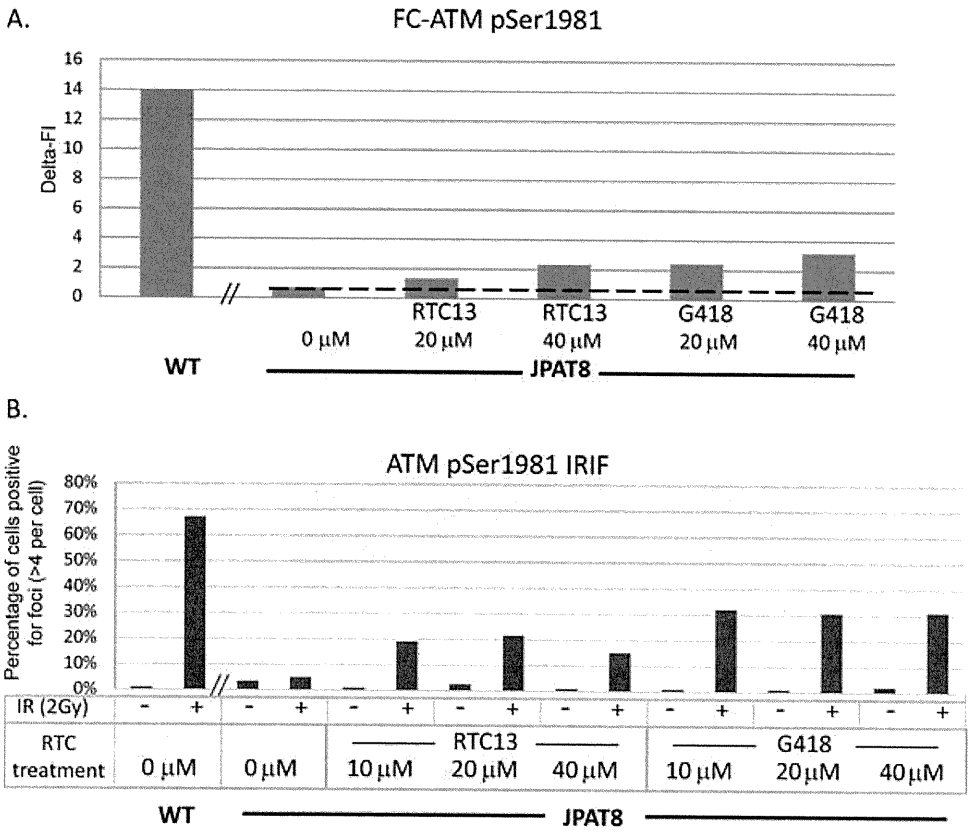

Figure 6. Readthrough compounds (RTCs) restored ATMpSer1981 autophosphorylation in JPAT8 LCL with a nonsense mutation. Cells were treated with readthrough compounds RTC13 and G418 for 4 days and then analyzed for ATMpSer1981. **(A)** ATMpSer1981 autophosphorylation level measured by FC-ATMpSer1981. Delta FI (fluorescence intensity) reflects the difference in FI between nonirradiated and irradiated cells. The data represent one of three independent experiments and results were consistent. **(B)** ATMpSer1981 foci formation by IRIF assay. The data are an average of two independent experiments.

LGDs and duplications within the *ATM* gene account for approximately 2% of reported mutations [Cavalieri et al., 2006, 2008; Coutinho, et al., 2004; Ejima and Sasaki, 1998; Gilad et al., 1996b; Mitui et al., 2003; Telatar et al., 1998b]. Few LGDs have been found in a homozygous state in A-T patients [Mitui et al., 2003]. The recent introduction of the MLPA technique has greatly improved the detection of genomic rearrangement mutations, including LGD and duplications in the *ATM* gene [Cavalieri et al., 2008].

Using MLPA, we identified the c.8851-2kbdel17kb mutation in JPAT3. While it was possible that this LGD mutation was ancestrally related to the previously reported CRAT [B] [Telatar et al., 1998a] and BRAT3 [Mitui et al., 2003] mutations, this now seems unlikely, since all three alleles are carried on different STR haplotypes. Given that homology between repetitive sequences is thought to underlie the formation of some genomic deletions and duplications [Kazazian and Goodier, 2002; Telatar et al., 1998a], we carried out an in silico analysis of DNA sequences flanking genomic deletions and were able to identify several repetitive sequences. The presence of microhomology (GGA in JPAT11) suggests that the recently described microhomology-mediated break-induced replication FoSTeS/MMBIR mechanism could be responsible for generating these deletions [Hastings et al., 2009].

Readthrough of PTCs was first described almost 50 years ago when it was noticed that certain aminoglycosides, such as streptomycin and gentamicin, "suppressed" the mutated phenotype of auxotrophy in strains of *Escherichia coli* suggesting that the drug interfered with accurate translation of the RNA code into protein [Davies et al., 1965]. Later, crystallography studies elegantly demonstrated that aminoglycosides bind to the internal loop of helix 44 (the decoding site) of the 16 S ribosomal RNA [Dibrov et al., 2010; Lynch et al., 2003]. More recently, we identified two new nonaminoglycoside small molecules with readthrough activity on both *ATM* and *dystrophin* genes [Du et al., 2009].

Based on the mutation spectrum of *ATM*, it is estimated that approximately 30% of *ATM* mutations in A-T patients are potentially treatable by mutation-targeted therapy using either RTCs or AMOs. This includes A-T patients who are compound heterozygotes, since RTCs and AMOs restore significant amounts of ATM protein even when only one allele is targeted. We identified three such examples amongst the eight Japanese families. In fact, in vitro, we were able to correct (1) abnormal splicing for JPAT11/12 (Fig. 5A), using a custom-designed AMO to mask the cryptic splice site created by the pseudoexon mutation (c.2639-384A>G); (2) a nonsense mutation in cells from JPAT8/9 using RTCs (Fig. 6). Thus, our results demonstrate that mutation-targeted treatment of cells carrying poorly understood DNA variants can extend our understanding of the consequences of such changes and may also have important therapeutic potential.

Acknowledgments

S.C. received a fellowship from "Associazione Gli Amici di Valentina." We thank Drs. Shareef Nahas, Hailiang Hu, and Mark Ambrose for helpful discussions.

References

Babushok DV, Kazazian HH, Jr. 2007. Progress in understanding the biology of the human mutagen LINE-1. Hum Mutat 28:527–539.

Bakkenist CJ, Kastan MB. 2003. DNA damage activates ATM through intermolecular autophosphorylation and dimer dissociation. Nature 421:499–506.

Birrell GW, Kneebone K, Nefedov M, Nefedova E, Jartsev MN, Mitsui M, Gatti RA, Lavin MF. 2005. ATM mutations, haplotype analysis, and immunological status of Russian patients with ataxia telangiectasia. Hum Mutat 25:593–601.

Boder E, Sedgwick RP. 1958. Ataxia-telangiectasia; a familial syndrome of progressive cerebellar ataxia, oculocutaneous telangiectasia and frequent pulmonary infection. Pediatrics 21:526–554.

Bolderson E, Richard DJ, Zhou BB, Khanna KK. 2009. Recent advances in cancer therapy targeting proteins involved in DNA double-strand break repair. Clin Cancer Res 15:6314–6320.

Broeks A, de Klein A, Floore AN, Muijtjens M, Kleijer WJ, Jaspers NG, van 't Veer LJ. 1998. ATM germline mutations in classical ataxia-telangiectasia patients in the Dutch population. Hum Mutat 12:330–337.

Campbell C, Mitui M, Eng L, Coutinho G, Thorstenson Y, Gatti RA. 2003. ATM mutations on distinct SNP and STR haplotypes in ataxia-telangiectasia patients of differing ethnicities reveal ancestral founder effects. Hum Mutat 21:80–85.

Cartegni L, Wang J, Zhu Z, Zhang MQ, Krainer AR. 2003. ESEfinder: a web resource to identify exonic splicing enhancers. Nucleic Acids Res 31:3568–3571.

Cavalieri S, Funaro A, Pappi P, Migone N, Gatti RA, Brusco A. 2008. Large genomic mutations within the ATM gene detected by MLPA, including a duplication of 41 kb from exon 4 to 20. Ann Hum Genet 72(Pt 1):10–18.

Cavalieri S, Funaro A, Porcedda P, Turinetto V, Migone N, Gatti RA, Brusco A. 2006. ATM mutations in Italian families with ataxia telangiectasia include two distinct large genomic deletions. Hum Mutat 27:1061–1070.

Coutinho G, Mitui M, Campbell C, Costa Carvalho BT, Nahas S, Sun X, Huo Y, Lai CH, Thorstenson Y, Tanouye R, Raskin S, Kim CA, Llerena J Jr, Gatti RA. 2004. Five haplotypes account for fifty-five percent of ATM mutations in Brazilian patients with ataxia telangiectasia: seven new mutations. Am J Med Genet A 126:33–40.

Davies J, Gorini L, Davis BD. 1965. Misreading of RNA codewords induced by aminoglycoside antibiotics. Mol Pharmacol 1:93–106.

Dibrov SM, Parsons J, Hermann T. 2010. A model for the study of ligand binding to the ribosomal RNA helix h44. Nucleic Acids Res 38:4458–4465.

Du L, Damoiseaux R, Nahas S, Gao K, Hu H, Pollard JM, Goldstine J, Jung ME, Henning SM, Bertoni C, Gatti RA. 2009. Nonaminoglycoside compounds induce readthrough of nonsense mutations. J Exp Med 206:2285–2297.

Du L, Kayali R, Bertoni C, Fike F, Hu H, Iversen PL, Gatti RA. 2011. Arginine-rich cell-penetrating peptide dramatically enhances AMO-mediated ATM aberrant splicing correction and enables delivery to brain and cerebellum. Hum Mol Genet 20:3151–3160.

Du L, Lai CH, Concannon P, Gatti RA. 2008. Rapid screen for truncating ATM mutations by PTT-ELISA. Mutat Res 640:139–144.

Du L, Pollard JM, Gatti RA. 2007. Correction of prototypic ATM splicing mutations and aberrant ATM function with antisense morpholino oligonucleotides. Proc Natl Acad Sci USA 104:6007–6012.

Ejima Y, Sasaki MS. 1998. Mutations of the ATM gene detected in Japanese ataxia-telangiectasia patients: possible preponderance of the two founder mutations 4612del165 and 7883del5. Hum Genet 102:403–408.

Eng L, Coutinho G, Nahas S, Yeo G, Tanouye R, Babaei M, Dork T, Burge C, Gatti RA. 2004. Nonclassical splicing mutations in the coding and noncoding regions of the ATM Gene: maximum entropy estimates of splice junction strengths. Hum Mutat 23:67–76.

Fukao T, Song XQ, Yoshida T, Tashita H, Kaneko H, Teramoto T, Inoue R, Katamura K, Mayumi M, Hiratani M and others. 1998. Ataxia-telangiectasia in the Japanese population: identification of R1917X, W2491R, R2909G, IVS33+2T->A, and 7883del5, the latter two being relatively common mutations. Hum Mutat 12:338–343.

Gatti RA. 2001. Ataxia-telangiectasia. In: Scriver CR, Beaudet AL, Sly WS, Valle D, editors. The Metabolic and Molecular Basis of Inherited Disease. Edition 8. New York: McGraw-Hill 677–704.

Gatti RA, Berkel I, Boder E, Braedt G, Charmley P, Concannon P, Ersoy F, Foroud T, Jaspers NG, Lange K and others. 1988. Localization of an ataxia-telangiectasia gene to chromosome 11q22–23. Nature 336:577–580.

Gilad S, Bar-Shira A, Harnik R, Shkedy D, Ziv Y, Khosravi R, Brown K, Vanagaite L, Xu G, Frydman M, and others. 1996a. Ataxia-telangiectasia: founder effect among north African Jews. Hum Mol Genet 5:2033–2037.

Gilad S, Khosravi R, Shkedy D, Uziel T, Ziv Y, Savitsky K, Rotman G, Smith S, Chessa L, Jorgensen TJ and others. 1996b. Predominance of null mutations in ataxia-telangiectasia. Hum Mol Genet 5:433–439.

Hastings PJ, Ira G, Lupski JR. 2009. A microhomology-mediated break-induced replication model for the origin of human copy number variation. PLoS Genet 5:e1000327.

Kazazian HH, Jr., Goodier JL. 2002. LINE drive. Retrotransposition and genome instability. Cell 110:277–280.

Kozlov SV, Graham ME, Peng C, Chen P, Robinson PJ, Lavin MF. 2006. Involvement of novel autophosphorylation sites in ATM activation. EMBO J 25:3504–3514.

Laake K, Telatar M, Geitvik GA, Hansen RO, Heiberg A, Andresen AM, Gatti R, Borresen-Dale AL. 1998. Identical mutation in 55% of the ATM alleles in 11 Norwegian AT families: evidence for a founder effect. Eur J Hum Genet 6:235–244.

Lai CH, Chun HH, Nahas SA, Mitui M, Gamo KM, Du L, Gatti RA. 2004. Correction of ATM gene function by aminoglycoside-induced read-through of premature termination codons. Proc Natl Acad Sci USA 101:15676–15681.

Lange E, Borresen AL, Chen X, Chessa L, Chiplunkar S, Concannon P, Dandekar S, Gerken S, Lange K, Liang T and others. 1995. Localization of an ataxia-telangiectasia gene to an approximately 500-kb interval on chromosome 11q23.1: linkage analysis of 176 families by an international consortium. Am J Hum Genet 57:112–119.

Liu HX, Cartegni L, Zhang MQ, Krainer AR. 2001. A mechanism for exon skipping caused by nonsense or missense mutations in BRCA1 and other genes. Nat Genet 27:55–58.

Lynch SR, Gonzalez RL, Puglisi JD. 2003. Comparison of X-ray crystal structure of the 30S subunit-antibiotic complex with NMR structure of decoding site oligonucleotide-paromomycin complex. Structure 11:43–53.

Matsuoka S, Ballif BA, Smogorzewska A, McDonald ER, 3rd, Hurov KE, Luo J, Bakalarski CE, Zhao Z, Solimini N, Lerenthal Y and others. 2007. ATM and ATR substrate analysis reveals extensive protein networks responsive to DNA damage. Science 316:1160–1166.

McConville CM, Stankovic T, Byrd PJ, McGuire GM, Yao QY, Lennox GG, Taylor MR. 1996. Mutations associated with variant phenotypes in ataxia-telangiectasia. Am J Hum Genet 59:320–330.

Minegishi Y, Saito M, Morio T, Watanabe K, Agematsu K, Tsuchiya S, Takada H, Hara T, Kawamura N, Ariga T and others. 2006. Human tyrosine kinase 2 deficiency reveals its requisite roles in multiple cytokine signals involved in innate and acquired immunity. Immunity 25:745–755.

Mitui M, Bernatowska E, Pietrucha B, Piotrowska-Jastrzebska J, Eng L, Nahas S, Teraoka S, Sholty G, Purayidom A, Concannon P and others. 2005. ATM gene founder haplotypes and associated mutations in Polish families with ataxia-telangiectasia. Ann Hum Genet 69(Pt 6):657–664.

Mitui M, Campbell C, Coutinho G, Sun X, Lai CH, Thorstenson Y, Castellvi-Bel S, Fernandez L, Monros E, Carvalho BT and others. 2003. Independent mutational events are rare in the ATM gene: haplotype prescreening enhances mutation detection rate. Hum Mutat 22:43–50.

Mitui M, Nahas SA, Du LT, Yang Z, Lai CH, Nakamura K, Arroyo S, Scott S, Purayidom A, Concannon P and others. 2009. Functional and computational assessment of missense variants in the ataxia-telangiectasia mutated (ATM) gene: mutations with increased cancer risk. Hum Mutat 30:12–21.

Morcos PA, Li Y, Jiang S. 2008. Vivo-Morpholinos: a non-peptide transporter delivers Morpholinos into a wide array of mouse tissues. Biotechniques 45:613–614, 616, 618 passim.

Morio T, Takahashi N, Watanabe F, Honda F, Sato M, Takagi M, Imadome K, Miyawaki T, Delia D, Nakamura K and others. 2009. Phenotypic variations between affected siblings with ataxia-telangiectasia: ataxia-telangiectasia in Japan. Int J Hematol 90:455–462.

Moulton JD, Jiang S. 2009. Gene knockdowns in adult animals: PPMOs and vivo-morpholinos. Molecules 14:1304–1323.

Nahas SA, Butch AW, Du L, Gatti RA. 2009. Rapid flow cytometry-based structural maintenance of chromosomes 1 (SMC1) phosphorylation assay for identification of ataxia-telangiectasia homozygotes and heterozygotes. Clin Chem 55:463–472.

Pattison JE. 2004. A comparison of inbreeding rates in India, Japan, Europe and China. HOMO—J Comp Hum Biol 55:113–128.

Savitsky K, Bar-Shira A, Gilad S, Rotman G, Ziv Y, Vanagaite L, Tagle DA, Smith S, Uziel T, Sfez S and others. 1995. A single ataxia telangiectasia gene with a product similar to PI-3 kinase. Science 268:1749–1753.

Schouten JP, McElgunn CJ, Waaijer R, Zwijnenburg D, Diepvens F, Pals G. 2002. Relative quantification of 40 nucleic acid sequences by multiplex ligation-dependent probe amplification. Nucleic Acids Res 30:e57.

Shiloh Y. 2006. The ATM-mediated DNA-damage response: taking shape. Trends Biochem Sci 31:402–410.

Smith PJ, Zhang C, Wang J, Chew SL, Zhang MQ, Krainer AR. 2006. An increased specificity score matrix for the prediction of SF2/ASF-specific exonic splicing enhancers. Hum Mol Genet 15:2490–2508.

Sobeck A. 2001. Caretaker-Gen-Syndrome:Molekulargenetische und Funktionelle Studien. PhD Thesis, Wuerzburg: Julius-Maximilians-University Wuerzburg.

Svedmyr EA, Leibold W, Gatti RA. 1975. Possible use of established cell lines for MLR locus typing. Tissue Antigens 5:186–195.

Telatar M, Teraoka S, Wang Z, Chun HH, Liang T, Castellvi-Bel S, Udar N, Borresen-Dale AL, Chessa L, Bernatowska-Matuszkiewicz E and others. 1998a. Ataxia-telangiectasia: identification and detection of founder-effect mutations in the ATM gene in ethnic populations. Am J Hum Genet 62:86–97.

Telatar M, Wang S, Castellvi-Bel S, Tai LQ, Sheikhavandi S, Regueiro JR, Porras O, Gatti RA. 1998b. A model for ATM heterozygote identification in a large population: four founder-effect ATM mutations identify most of Costa Rican patients with ataxia telangiectasia. Mol Genet Metab 64:36–43.

Teraoka SN, Telatar M, Becker-Catania S, Liang T, Onengut S, Tolun A, Chessa L, Sanal O, Bernatowska E, Gatti RA and others. 1999. Splicing defects in the ataxia-telangiectasia gene, ATM: underlying mutations and consequences. Am J Hum Genet 64:1617–1631.

Udar N, Farzad S, Tai LQ, Bay JO, Gatti RA. 1999. NS22: a highly polymorphic complex microsatellite marker within the ATM gene. Am J Med Genet 82:287–289.

Valentine CR. 1998. The association of nonsense codons with exon skipping. Mutat Res 411:87–117.

Vanagaite L, James MR, Rotman G, Savitsky K, Bar-Shira A, Gilad S, Ziv Y, Uchenik V, Sartiel A, Collins FS and others. 1995. A high-density microsatellite map of the ataxia-telangiectasia locus. Hum Genet 95:451–454.

Westbrook AM, Schiestl RH. 2010. Atm-deficient mice exhibit increased sensitivity to dextran sulfate sodium-induced colitis characterized by elevated DNA damage and persistent immune activation. Cancer Res 70:1875–1884.

Yeo G, Burge CB. 2004. Maximum entropy modeling of short sequence motifs with applications to RNA splicing signals. J Comput Biol 11:377–394.

OPEN ACCESS Freely available online

PLoS one

Onset of Quiescence Following p53 Mediated Down-Regulation of H2AX in Normal Cells

Yuko Atsumi[1☯], Hiroaki Fujimori[1,3☯], Hirokazu Fukuda[2☯], Aki Inase[2], Keitaro Shinohe[3], Yoshiko Yoshioka[3], Mima Shikanai[3], Yosuke Ichijima[3], Junya Unno[4], Shuki Mizutani[4], Naoto Tsuchiya[2], Yoshitaka Hippo[2], Hitoshi Nakagama[2], Mitsuko Masutani[1], Hirobumi Teraoka[3], Ken-ichi Yoshioka[1,3]*

1 Division of Genome Stability Research, National Cancer Center Research Institute, Tokyo, Japan, **2** Division of Cancer Development System, National Cancer Center Research Institute, Tokyo, Japan, **3** Department of Pathological Biochemistry, Medical Research Institute, Tokyo Medical and Dental University, Tokyo, Japan, **4** Department of Pediatrics and Developmental Biology, Graduate School of Medical and Dental Sciences, Tokyo Medical and Dental University, Tokyo, Japan

Abstract

Normal cells, both *in vivo* and *in vitro*, become quiescent after serial cell proliferation. During this process, cells can develop immortality with genomic instability, although the mechanisms by which this is regulated are unclear. Here, we show that a growth-arrested cellular status is produced by the down-regulation of histone H2AX in normal cells. Normal mouse embryonic fibroblast cells preserve an H2AX diminished quiescent status through p53 regulation and stable-diploidy maintenance. However, such quiescence is abrogated under continuous growth stimulation, inducing DNA replication stress. Because DNA replication stress-associated lesions are cryptogenic and capable of mediating chromosome-bridge formation and cytokinesis failure, this results in tetraploidization. Arf/p53 module-mutation is induced during tetraploidization with the resulting H2AX recovery and immortality acquisition. Thus, although cellular homeostasis is preserved under quiescence with stable diploidy, tetraploidization induced under growth stimulation disrupts the homeostasis and triggers immortality acquisition.

Citation: Atsumi Y, Fujimori H, Fukuda H, Inase A, Shinohe K, et al. (2011) Onset of Quiescence Following p53 Mediated Down-Regulation of H2AX in Normal Cells. PLoS ONE 6(8): e23432. doi:10.1371/journal.pone.0023432

Editor: Michael Polymenis, Texas A&M University, United States of America

Received April 11, 2011; **Accepted** July 17, 2011; **Published** August 12, 2011

Funding: This study was supported by MEXT KAKENHI (20770136 and 20659047). The funders had no role in study design, data collection and analysis, decision to publish, or preparation of the manuscript.

Competing Interests: The authors have declared that no competing interests exist.

* E-mail: kyoshiok@ncc.go.jp

☯ These authors contributed equally to this work.

Introduction

Cancer is a disease associated with genomic instability and the accumulation of mutations [1]. Unlike specific chromosomal translocation-associated tumors, most cancers associated with aging develop either chromosomal instability (CIN) or microsatellite instability (MIN) [2]. While MIN is associated with mismatch repair deficiency, CIN develops even in a normal background [3]. However, the mechanisms by which CIN and MIN develop remain elusive.

A recent genomic analysis of various cancers revealed that massive genomic rearrangements, including loss of heterozygosity (LOH) and chromosomal translocation, amplification and deletion, do not gradually accumulate over time, as conventionally thought, but appear to be acquired in a single catastrophic event [4]. One of such events could be associated with tetraploidization because tetraploidy is a common early event in cancer cells with CIN [5]. Tetraploidy is observed in cells during the initial stages of cancer [6,7] as well as in precancerous stages such as dysplasia [8,9], but not in malignant cancer cells, which usually exhibit aneuploidy in association with deploidization [5]. Furthermore, analogous to changes observed in cancer genomes, the immortalization of mouse embryonic fibroblasts (MEFs) occurs with tetraploidy and mutation of the Arf/p53 module, which eventually evolves into aneuploidy during serial cultivation [10].

In the initial stages of carcinogenesis, cells are subjected to oncogenic stress, resulting in the accumulation of DNA replication stress-associated lesions and the onset of barrier responses such as senescence and apoptosis [11,12]. This effect can be reproduced *in vitro* by the activation of oncogenes [11] and accelerated growth stimulation [12] due to the induction of accelerated S-phase entry and the resulting DNA replication stress. Importantly, genomic instability is generated under these conditions [11,12] because DNA replication stress-associated lesions persist into M phase and mediate chromosomal bridge formation and cytokinesis failure, resulting in tetraploidization [10]. In fact, tetraploidization of MEFs is induced via chromosomal bridge formation prior to the onset of immortality with mutation of Arf/p53 [10], although it is still unclear how tetraploidization induces immortality. Since such tetraploidization is specifically observed during senescence, tetraploidization might be a defect that occurs during cell proliferation or growth arrest. In fact, similar to cells in the initial stages of carcinogenesis, senescent cells often accumulate irreparable DNA lesions [13,14] and frequently exhibit genomic instability [15].

The development of cancer, as well as the onset of immortality in cells *in vitro*, is tightly associated with mutations in the Arf/p53 module [16–18]. Although this is ascribed to the role of p53 in

cancer prevention, the regulation and roles of p53 are complex [18]. While constitutively active p53 mediates premature aging in mice [19–21], additional single gene copies of *Arf* and *p53* under functional regulation mediate longevity and cancer prevention [22]. Similarly, while the accumulation of p53 induces cellular senescence and apoptosis [16,17], additional single gene copies of *Arf* and *p53* in MEFs has a protective effect from immortalization [22], suggesting that they help to maintain homeostasis under undamaged conditions. This raises the questions of the identity of the regulatory target of p53 in preserving cellular homeostasis under normal conditions and how cellular homeostasis preservation and abrogation are associated with genomic status and p53 regulation.

This study focused on the mechanism by which normal cells under serial proliferation regulate homeostasis preservation and abrogation and sought to identify the regulatory target of p53. Our results illustrated two distinct conditions that could result in growth-arrested cells: (i) cells that maintain continuous quiescence by down-regulating H2AX (a variant of core histone H2A) under p53 regulation and stable-diploidy maintenance; and (ii) cells that develop tetraploidy and immortality under continuous growth stimulation, characterized by the accumulation of γH2AX foci. Thus, oncogenic stress under growth stimulation triggers catastrophic tetraploidization that leads to immortalization in association with the accompanying mutation of the Arf/p53 module and recovery of H2AX expression and growth activity.

Results

Immortality is prevented in quiescent cells that maintain genomic stability

MEFs cultured under the standard 3T3 protocol (Std-3T3) senesce in association with oxygen sensitivity [23], which is followed by the development of immortality with tetraploidy [10] and mutation of the Arf/p53 module [22], similar to the process of carcinogenesis. In addition, similar to cells in the initial stages of carcinogenesis, spontaneous DNA lesions accumulate in senescent MEFs under Std-3T3 conditions prior to the development of immortality [10], which suggests that growth stimulation induced under Std-3T3 conditions might overwhelm senescent MEFs. Therefore, MEFs under Std-3T3 conditions were compared with MEFs exposed to temporary serum deprivation (tSD-3T3), which induces occasional growth arrest (Fig. 1A). Under Std-3T3 conditions, MEFs were immortalized with tetraploidy that progresses to aneuploidy (Fig. 1A–C). On the other hand, MEFs cultured under tSD-3T3 conditions never developed immortality and preserved quiescence with stable diploidy (Fig. 1A, C). This indicates that temporal growth arrest prevents immortalization and supports genomic stability. Conversely, continuous culture with 10% FBS produces oncogenic stress in senescent MEFs, triggering tetraploidization. Thus, even though both are growth arrested (at least in total cell numbers) with senescent morphology at the same culture passage (P9) (Fig. S1), MEFs under tSD-3T3 conditions are continuously quiescent with genomic stability, while MEFs under Std-3T3 conditions develop tetraploidy (Fig. 1A, C), posing a question in DNA lesion status that induces chromosomal bridge formation and tetraploidization [10].

γH2AX foci accumulate in cells developing genomic instability but not in cells preserving diploidy

To determine the DNA lesion status induced by accelerated growth stimulation, γH2AX foci were compared in growth-arrested MEFs (P9) under both conditions (Fig. 1D). As expected, MEFs that developed tetraploidy under Std-3T3 conditions accumulated γH2AX foci, with some carrying over into the G2/M phases (Fig. 1E). This resulted in chromosome bridge formation (Fig. 1F) with the resulting tetraploidization that is initially observed with binucleated tetraploidy (Fig. 1F). On the other hand, quiescent MEFs that preserved genomic stability under tSD-3T3 conditions did not develop γH2AX foci (Fig. 1D), indicating that genomic stability is preserved under no γH2AX signal. However, it was still unclear why quiescent MEFs under tSD-3T3 conditions do not accumulate γH2AX foci because senescent cells are known to generally accumulate irreparable DNA lesions [13,14].

To address why γH2AX foci do not form under tSD-3T3 conditions, the expression level of H2AX at P9 was determined. As shown in Figure 1G, a remarkable reduction in H2AX expression was observed in quiescent MEFs at P9 while MEFs that developed tetraploidy under Std-3T3 conditions showed significantly higher H2AX expression than quiescent MEFs. This illustrates an association between H2AX levels and the cellular and genomic status, in that cells with largely diminished H2AX expression preserve stable diploidy and a quiescent status, while cells with residual H2AX expression and with γH2AX foci develop genomic instability and immortality (Fig. 1H). Importantly, H2AX-KO cells exhibited impaired DNA repair, growth retardation, and elevated genomic instability [24–28], phenotypes reminiscent of senescent cells. Therefore, it will be critical to determine how H2AX-status is regulated to produce quiescence and induce genomic instability.

H2AX is generally diminished in quiescent cells

To address whether H2AX diminution is a general occurrence, H2AX expression was compared in normal human fibroblasts (NHFs) and MEFs. Decreased H2AX was observed in both cell types at growth-arrested stage after serial proliferation (Fig. 2A, B), suggesting that this process is conserved between humans and mice. In addition, H2AX diminution was also observed in many organs of adult mice, including the liver, spleen, and pancreas (Fig. 2C, D; Fig. S2). Thus, H2AX is generally reduced in quiescent cell chromosomes both *in vitro* and *in vivo*.

H2AX is also diminished during premature senescence induced by DNA damage. Using early passage MEFs (P2), H2AX diminution was observed when senescence was induced by treatment with hydroxyurea (HU) to induce DNA replication stress (Fig. 2E) and with the radiomimetic DNA-damaging agent, neocarzinostatin (Fig. S3). This most likely occurs because DNA repair is coupled with H2AX release and chromatin remodeling [29–31]. Together with results showing a decrease in H2AX transcript levels in senescent MEFs (Fig. S4), these results indicate that decreased amounts of H2AX protein in senescing cells is ascribed to a decrease in H2AX transcript levels and DNA damage.

To directly address the impact of H2AX reduction, H2AX was knocked down in early passage NHFs, which induced cellular quiescence with senescent cell characteristics; cells adopted a flattened and enlarged morphology and showed an increase in senescence-associated β-galactosidase activity (Fig. 2F). Since the knockdown of H2AX in 293T cells induced growth arrest without inducing a senescent morphology (data not shown), it is likely that the effect of H2AX diminution is primarily due to quiescence induction and potentially a normal consequence of senescence in normal cells.

Immortalized cells develop following tetraploidization when H2AX status and growth activity are restored

The above results illustrate that cellular quiescence is produced when cells maintain stable diploidy and diminished H2AX

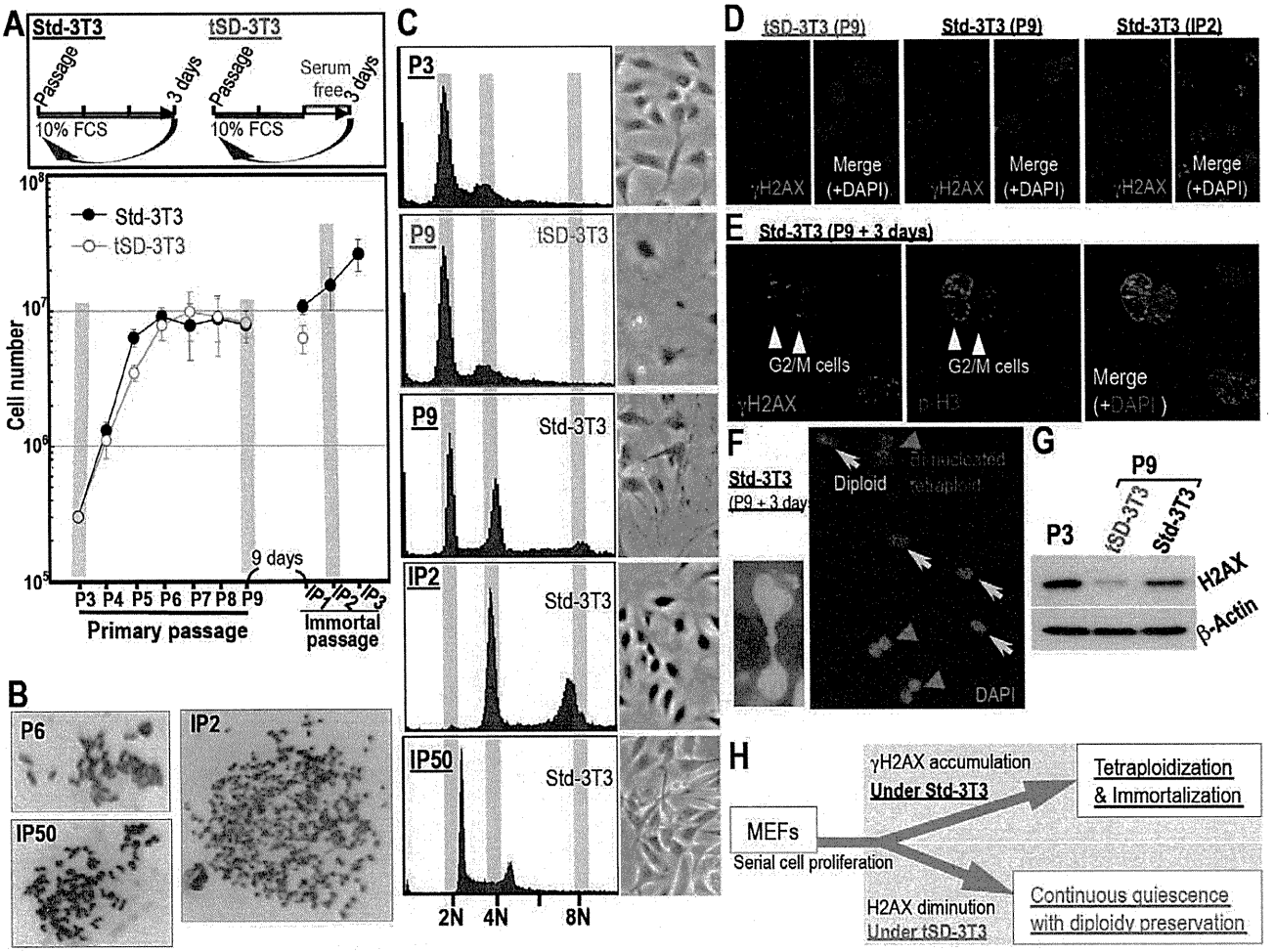

Figure 1. Immortality with tetraploidy is blocked in quiescent cells with diploidy, diminished H2AX, and no γH2AX foci. A. Growth curves of MEFs cultured under the standard 3T3 protocol (Std-3T3) or the T3 protocol with temporary serum deprivation (tSD-3T3) as schematically shown. MEFs under Std-3T3 conditions were immortalized, whereas MEFs cultured under tSD-3T3 conditions were not. **B** Genomic instability developed in immortalized MEFs (IP2) under Std-3T3 conditions. **C.** Genomic status was determined by flow-cytometry at the indicated conditions and passages. Representative images are shown. Tetraploidy development was blocked under tSD-3T3 conditions, while tetraploidy had already developed in growth-arrested MEFs at P9 under Std-3T3 conditions (see increasing 4N and 8N peaks). **D.** DNA lesions identified by γH2AX foci spontaneously accumulated in MEFs developing tetraploidy and immortality (P9) under Std-3T3 conditions as well as in immortal cells (IP2), while MEFs that maintained quiescent status with genomic stability under tSD-3T3 conditions contained no foci. **E.** DNA lesion-carryover into the G2-M phases was determined for lesions that spontaneously accumulated in senescent MEFs under Std-3T3 conditions. DNA lesions in senescing MEFs are also observed in the G2-M phases determined by phosphorylated H3. **F.** Chromosome bridge formation (Left panel) is observed in association with DNA lesion-carryover into the G2-M phases under Std-3T3 conditions with the resulting accumulation of bi-nucleated tetraploidy (Right panel: red arrow heads). Representative images are shown. **G.** The total H2AX level at P9 under each condition was determined. Whereas a significant reduction in H2AX expression was observed in MEFs with genomic stability under tSD-3T3 conditions, MEFs that developed immortality and genomic instability under Std-3T3 conditions did not show a significant decrease in H2AX expression. **H.** A model of the life-cycle of MEFs undergoing quiescence or developing immortality. While quiescent MEFs preserve diploidy and show diminished H2AX levels, MEFs developing immortality exhibited γH2AX foci accumulation.

doi:10.1371/journal.pone.0023432.g001

expression. In these cells, the H2AX level is less than 100-fold compared to that in actively growing cells. To study the effect of growth stimulation in cells with an H2AX-diminished quiescent status, complete medium (DMEM with 10% FBS) was added to quiescent MEFs prepared under tSD-3T3 conditions (Fig. 3A–C). In these cells, cell-cycle progression was initiated with the expression of PCNA and histones H3 and H2AX, which led to γH2AX foci formation (Fig. 3D, E). Abrogating quiescent status with complete medium resulted in the establishment of immortalized MEFs with tetraploidy (Fig. 3A–C). However, it took 30 days to initiate immortal passage in H2AX-diminished quiescent MEFs, while immortality was acquired in only 9 days for P9 MEFs under Std-3T3 conditions, suggesting that the H2AX-diminished quiescent status protected cells from immortalization. Supporting this argument, primary MEFs transfected with an H2AX expression vector also acquired immortality at an accelerated rate (Fig. S5A–C). Such H2AX-overexpression may induce the effect of DNA replication stress because immortality in H2AX-overexpressing MEFs were again developed with tetraploidy (Fig. S5D,E). Unexpectedly, H2AX status was totally recovered in actively growing, immortalized MEFs (Fig. 3F, G), which illustrates the association of H2AX status with growth activity.

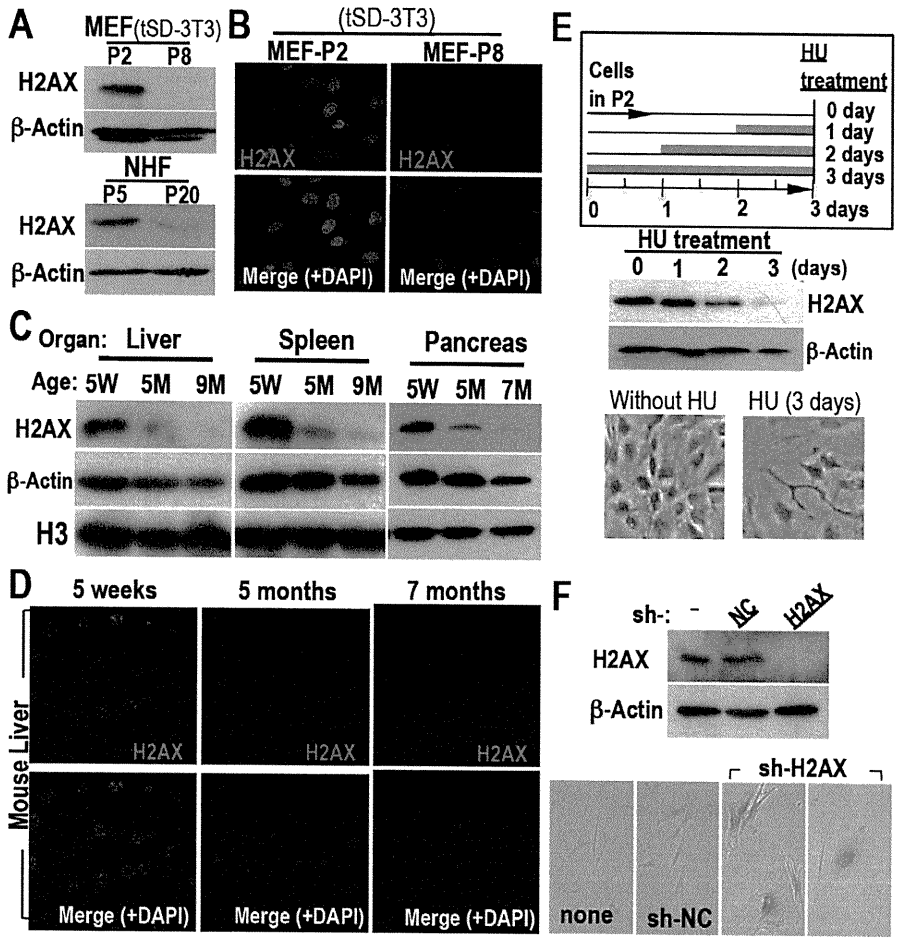

Figure 2. Quiescent cell-status is induced with H2AX diminution both *in vitro* and *in vivo*. A,B H2AX expression in growth-arrested cells (P8 for MEFs under tSD-3T3 conditions, P20 for NHFs) was determined by Western blotting (**A**) and immunofluorescent staining (**B**), revealing H2AX diminution in both types of growth-arrested cells. **C,D** H2AX diminution was also measured in adult mice organs by Western blotting (**C**) and in liver sections by immunofluorescent staining (**D**). Samples were prepared from five week (5W), five month (5M) and seven- or nine-month-old mice (7M or 9M). **E.** The involvement of H2AX diminution in DNA damage-induced premature senescence was determined after 0.2 mM HU treatment. Orange bars indicate the periods of HU treatment. Premature damage-induced senescence was observed with H2AX diminution, in which cells were flattened and enlarged, morphology typical of senescent cells. **F.** The effect of H2AX knockdown on senescence was determined in NHFs. Senescence was directly induced by H2AX knockdown in NHFs. H2AX status and senescence was determined by Western blotting (top) and SA-β-gal activation, and cells exhibited a flattened and enlarged morphology (bottoms), respectively.
doi:10.1371/journal.pone.0023432.g002

However, this also poses the question of how the down-regulation of H2AX expression in quiescent MEFs is reversed after immortalization.

Immortalized cells no longer achieve H2AX diminution-associated quiescent status

To explore the effects of the change in H2AX status, the response of H2AX to DNA replication stress was compared between primary and immortalized MEFs. While H2AX in primary MEFs was down-regulated after HU treatment, this did not occur in immortalized MEFs (Fig. 3H), which indicates that H2AX diminution-associated quiescent cell status is not inducible after immortalization. Thus, quiescent status is preserved in cells with diminished H2AX expression and stable diploidy but is abrogated under continuous growth stimulation, inducing cell cycle progression and γH2AX foci formation, and eventually leading to immortality with tetraploidy and H2AX recovery. Since the Arf/p53 module is specifically mutated during MEF immortalization [22], p53 might be involved in H2AX down-regulation. In fact, unlike senescent normal cells, H2AX expression is relatively high (2–20% of total H2A) in cancer cells as well as in growing NHFs (10%) [28].

H2AX diminution-associated quiescent status is produced by p53 and prohibits the development of immortality

To determine the involvement of p53 in H2AX down-regulation, *p53* knockout (KO) MEFs were cultured. Unlike normal primary MEFs, but similar to immortalized MEFs (Fig. 3H), H2AX expression in primary *p53*-KO-MEFs was not decreased by HU treatment (Fig. 4A). Furthermore, *p53*-KO-MEFs continuously grew, without change in H2AX status even under tSD-3T3 conditions (Fig. 4B, C). This indicates that H2AX in wild-type (WT)-MEFs is down-regulated by p53 to

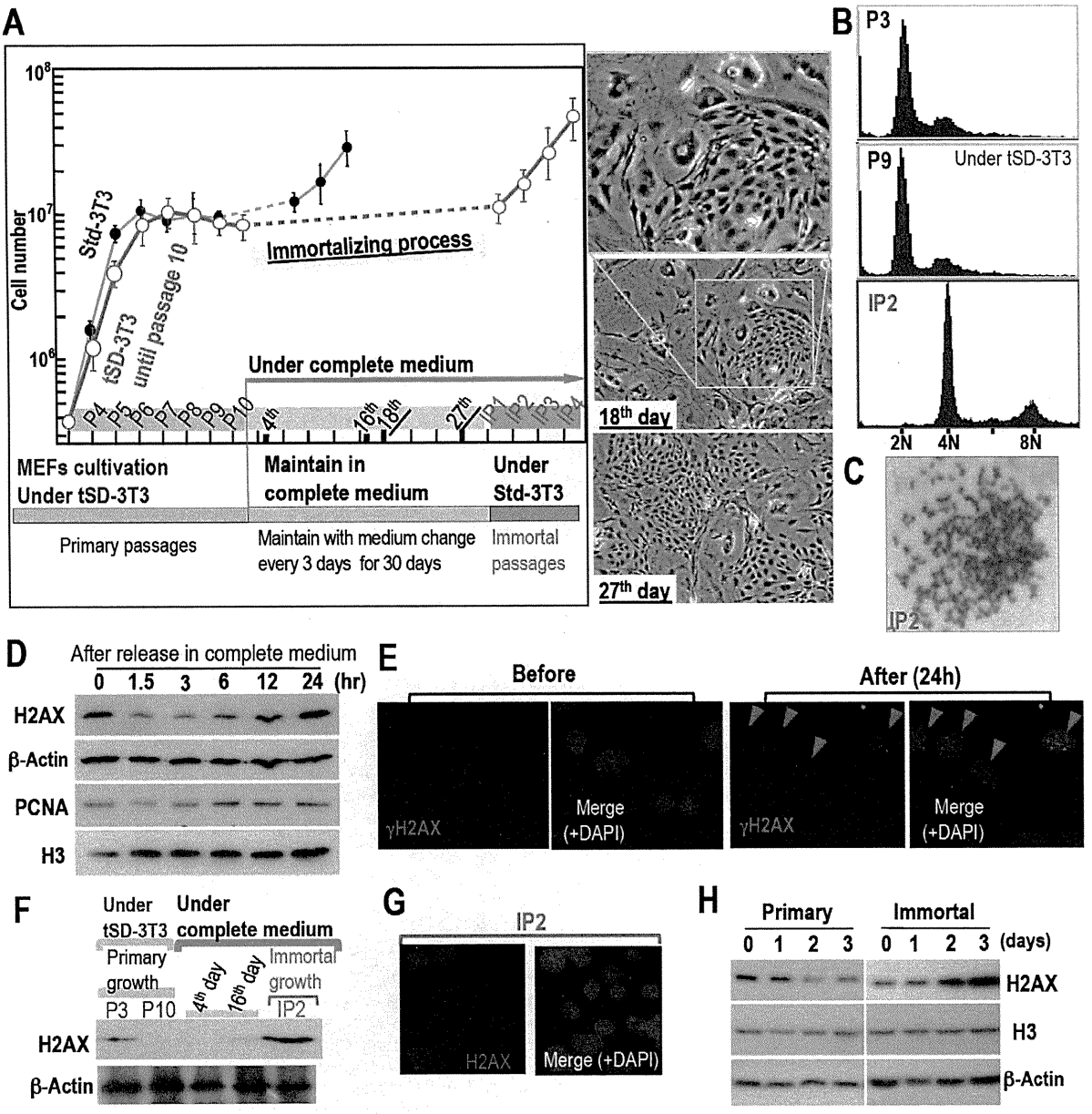

Figure 3. H2AX-diminished quiescent cell-status is abolished by continuous growth stimulation with accompanying H2AX recovery. A. Quiescent MEFs with diminished H2AX expression were cultured under tSD-3T3 conditions until P10. They were then exposed to complete medium, which was changed every three days for 30 days. Immortal passages were started under Std-3T3 conditions (red circles). MEFs cultured under the Std-3T3 conditions (black circles) as in Figure 1a were superimposed for comparison of the time needed to acquire immortality. Representative images of MEFs during the process of acquiring immortality are also shown. **B,C.** Tetraploidy development in immortalized MEFs (IP2) was observed by flow-cytometry (**B**) and Giemsa staining (**C**). **D.** Growth acceleration-associated cell cycle progression and H2AX induction. To determine the effect of serum induction on H2AX expression and cell cycle progression, senescent MEFs at P8 were incubated in serum-free medium for 24 h and harvested after exposure to complete medium for various times. H2AX expression increased with increasing PCNA and histone H3, which suggests that the expression of these chromatin factors was associated with S phase entry. To detect H2AX levels in these MEFs at P8, the H2AX signal was visualized by longer exposure. **E.** DNA lesions characterized by γH2AX foci were induced in MEFs (red arrowheads) after exposure to complete medium as in **D**. **F,G.** H2AX status in immortalized MEFs was determined by Western blotting (**F**) and immunofluorescence (**G**), revealing H2AX recovery. **H.** DNA replication stress-associated H2AX diminution was compared between normal and immortalized MEFs as in Figure 2E, in which H2AX was not down-regulated after immortalization.
doi:10.1371/journal.pone.0023432.g003

induce cellular quiescence and is recovered in immortalized MEFs in association with tetraploidization and mutation of the Arf/p53 module. Although *p53*-KO-MEFs did not undergo H2AX diminution-mediated growth arrest, these MEFs still exhibited a senescent morphology (Fig. 4D, see P8) and subsequently achieved an immortalized morphology (P14), which suggests the immortalization of *p53*-KO-MEFs via the senescent stage without growth arrest. This also indicates that a quiescent cell status is induced by p53 to protect cells from immortality.

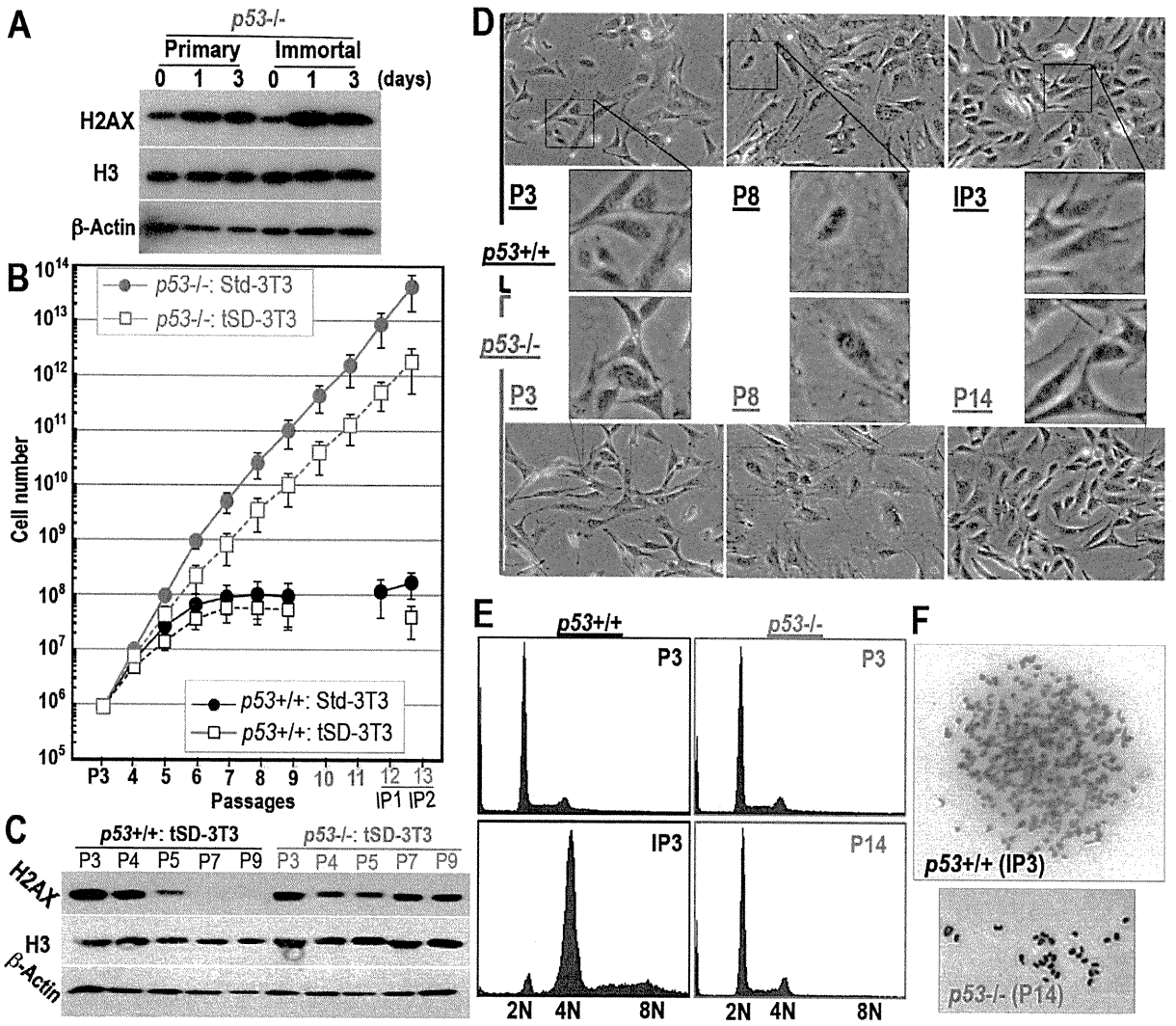

Figure 4. H2AX-diminished quiescent cell status is regulated by p53. A. DNA replication stress-associated H2AX diminution status was determined in *p53*-KO MEFs as in Figure 2E, in which H2AX was not down-regulated, even in primary MEFs. **B–F.** Primary *p53*-KO MEFs were cultured during the senescing and immortalizing processes (**B**). H2AX status was determined by Western blotting (**C**), morphological assessment (**D**), genomic status determined by flow-cytometry (**E**), and chromosome spread (**F**). Although *p53*-KO MEFs never showed major changes in H2AX expression, tetraploidization or growth arrest, *p53*-KO MEFs still exhibited a senescent morphology (P8) before achieving an immortalized morphology (P14).
doi:10.1371/journal.pone.0023432.g004

Mutation of the Arf/p53 module is induced with tetraploidization, triggered by DNA replication stress under moderately decreased H2AX levels in normal cells

Whereas *p53*-KO-MEFs are immortalized with diploidy (Fig. 4E, F), WT-MEFs are never immortalized only after tetraploidization [10] (Fig. 1B, C; Fig. 3B, C; Fig. 4E, F) and loss of Arf/p53 [22]. This suggests that the mutation of the Arf/p53 module in WT-MEFs is induced during tetraploidization. Supporting this argument, p53-dependent quiescence produced by diminished H2AX is maintained under diploidy preservation but abrogated after tetraploidization with mutation in the Arf/p53 module and the resulting H2AX recovery (Fig. 3). Therefore, normal WT-MEFs are protected from immortalization by a quiescent cell status, as long as the genome is preserved in diploidy. However, under continuous growth stimulation, tetraploidization also spontaneously arises in WT-MEFs but, unexpectedly, not in *p53*-KO-MEFs.

As tetraploidization was observed at the senescent stage under conditions of continuous growth stimulation that induce DNA replication stress (Fig. 3), the underlying reason for tetraploidization in WT-MEFs but not in *p53*-KO-MEFs might be associated with the repair deficiency that also occurs in an H2AX-diminished background. To examine the tetraploidization risk under an H2AX-diminished background, MEFs of each type were treated with HU for 36 hours and the incidence of bi-nucleated tetraploidy formation was compared (Fig. 5A). As expected, HU treatment-associated H2AX diminution (Fig. 2E) resulted in tetraploidization in primary WT-MEFs but not in immortalized WT-MEFs or p53-KO-MEFs (Fig. 5A). Thus, although normal cells become quiescent with largely diminished H2AX under diploidy, senescing cells with residual H2AX under growth stimulating conditions are potentially at risk of developing tetraploidy in response to DNA replication stress.

Finally, to address changes in DNA replication stress-sensitivity during serial proliferation of normal MEFs, the repair efficiencies

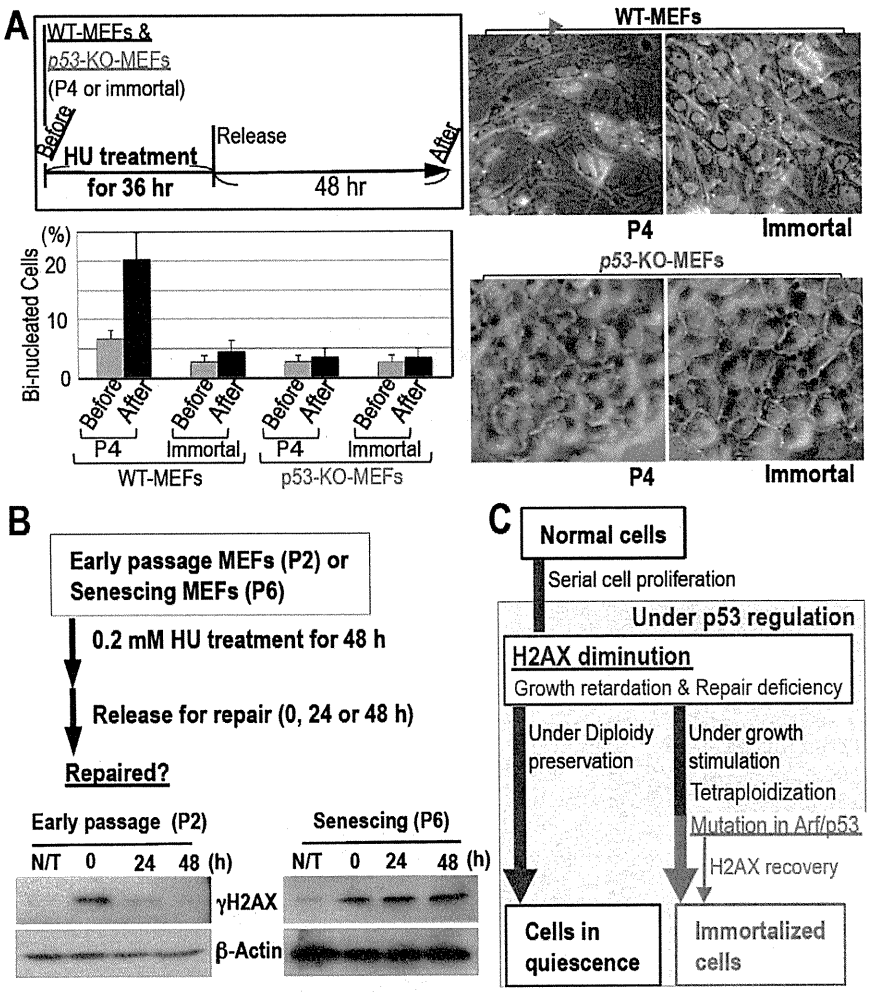

Figure 5. Increased risk of tetraploidization in normal MEFs. A. DNA replication stress-associated tetraploidization was determined in MEFs (P4) with the formation of bi-nucleated tetraploidy (red arrowhead) after 0.2 mM HU treatment as illustrated (top-left panel). Tetraploidization was efficiently induced during primary growth but not in immortalized MEFs or *p53*-KO-MEFs. **B.** Repair efficiencies of DNA replication stress-associated lesions were compared between early passage (P2) and senescing MEFs (P6) after 48 h hydroxyurea (HU) treatment. γH2AX signal was used as a marker of DNA lesions, in which γH2AX signal and β-Actin signals in senescing MEFs (P6) were detected only with over-exposure compared to early passage MEFs (P2), due to decreased H2AX levels during senescence. The reduction in γH2AX signal after release was only evident in early passage MEFs, which suggests that senescing cells are defective in resolving DNA replication stress. **C.** A model of MEFs under serial cell proliferation either undergoing quiescence or developing immortality. While MEFs that maintain quiescence and diploidy show diminished H2AX levels, MEFs developing immortality accumulate γH2AX foci.
doi:10.1371/journal.pone.0023432.g005

of DNA replication stress-associated lesions were compared between early passage and senescent MEFs with the decay of the γH2AX signal after release from HU treatment (Fig. 5B). Unlike early passage MEFs (P2), senescing MEFs (P6) were deficient in repairing HU-associated DNA lesions (Fig. 5B), in which MEFs show slow cell-cycle progression and residual H2AX expression. This is in contrast to quiescent MEFs with largely diminished H2AX level that show neither detectable cell cycle progression nor DNA replication stress. Thus, normal cells under serial proliferation decrease H2AX expression; thereby, cells slow growth activity and become defective in DNA repair. In such cells, cellular homeostasis is preserved by quiescence under largely diminished H2AX level regulated by p53 as long as diploidy is preserved. However, these cells are simultaneously at increased risk of tetraploidization with p53 dysfunction under continuous growth acceleration, resulting in the development of immortality and recovery of H2AX activity and cell growth (Fig. 5C).

Discussion

The results of this study revealed the following novel concepts: (i) normal cells generally achieve quiescent status with diminished H2AX level both *in vitro* and *in vivo*, and this is regulated by p53; (ii) growth arrested normal cells with senescent morphology can be defined as either (a) those in a continuous quiescent status with largely diminished H2AX level or (b) those in a transient status with inducing genomic instability and the resulting onset of immortality, under which cells accumulate γH2AX foci; (iii) to protect cells from immortality, one of the critical roles of p53 is the induction of growth-arrest via the down-regulation of H2AX with cellular quiescence. Cells in H2AX diminution-associated quiescence are shown in the cause of mature and premature senescence, during which cells show senescent morphology (Fig. S1), probably because these cells are repair defective (Fig. 5B). However such repair deficiency is also associated with genomic instability

development under accelerated growth stimulation, resulting in immortality acquisition with Arf/p53 module mutation and H2AX recovery.

Since growth-arrested cellular status with senescent morphology is directly induced by H2AX-knockdown (Fig. 2F), H2AX down-regulation is involved in a cause of quiescent cellular status. On the other hand, residual H2AX-expression in senescent cells is an associated effect for tetraploidization and immortalization: residual H2AX in senescent cells are only observed under accelerated growth stimulation (Figs. 1 and 3), under which cells are subjected to DNA replication stress and exhibit γH2AX, resulting in tetraploidization. Thus, even though cells are morphologically senescent with no growth in total cell number, cellular statuses could be either cells developing genomic instability under continuous growth acceleration (Std-3T3) or continuously quiescent cells under occasional arrest (tSD-3T3).

Unlike highly accumulated p53 that induces apoptosis, the Arf/p53 module under normal conditions functions for longevity by suppressing tumors in mice and giving protection from immortalization in MEFs [22]. Here, our results illustrated that such cellular status is produced with H2AX diminution-associated quiescence by protecting from immortalization under normal p53 regulation but is abrogated by Arf/p53 module mutation that is induced with tetraploidization under continuous growth stimulation, resulting in recovery of H2AX and growth activity. Unlike cells undergoing apoptosis, cells preserving quiescence under normal conditions do not accumulate p53 protein [10], which is probably associated with p53 function expression for quiescent status preservation but not for apoptosis induction. Intriguingly, such p53-dependent H2AX diminution was only observed after cells reach growth arrest both *in vivo* and *in vitro* but not growing cells in early passages and in organs from young mice (Fig. 2). In accordance with this, the expression of p53 targets Sidt2 and Phlda3, which are likely associated with tumor suppression [32], were elevated after cells become H2AX diminution-associated quiescent (P7) compared to cells in early passage (P3) (Fig. S6). However, similar to p53 protein, the increase in p53 transcript is also limited (Fig. S6). Thus, p53 function is expressed for apoptosis with accumulated p53, otherwise for H2AX-diminution associated quiescent status preservation under normal regulation without accumulating p53.

Except for tumors associated with specific chromosomal translocation, development of most cancers as well as *in vitro* cellular transformation is associated with genomic instability of either CIN or MIN [2,3]. Importantly, tetraploidization, a major initial form of CIN under a mismatch repair proficient background is induced with oncogenic stress by accelerated S-phase entry [10], leading to immortality acquisition in MEFs with mutation in the Arf/p53 module. Here, our results showed that quiescence could be preserved with largely diminished H2AX and diploidy preservation under the regulation of p53. Although H2AX down-regulation is only observed under functional p53 regulation, it is still unclear how p53 down-regulates H2AX. Our results showed the reduction of total H2AX transcript during the senescing process (Fig. S4) and a damage-induced decrease of H2AX protein under functional p53 regulation (Fig. 2E; Fig. 4A, B). Although p53 role for H2AX down-regulation is unclear, the regulation might be indirect because (1) there is no p53-binding site on the *H2AX* promoter, (2) there is no signal of the *H2AX* gene with ChIP-on-CHIP analyses against p53 [33], (3) H2AX expression does not associate with the activation level of p53 as we observed no association between H2AX expression and p53 activation (Fig. S7).

Together, our results provide a rationale for the regulation of cellular homeostasis preservation. By prohibiting immortality development and preserving quiescent cell status, p53 induces an H2AX diminution-mediated quiescent status. However, this status is abrogated by continuous growth stimulation, which results in the induction of genomic instability with mutation of the Arf/p53 module, which leads into H2AX recovery, the restoration of growth activity, and immortality acquisition (Fig. 5C).

Methods

Ethics Statement

Mice were treated in accordance with the Japanese Laws and the Guidelines for Animal Experimentation of National Cancer Center. All experiments were approved by The Committee for Ethics in Animal Experimentation of National Cancer Center (approval ID numbers: A59-09 and T07-038).

Cell culture and tissue samples

Cells were cultured as described previously [34]. Both wild-type and *p53*-KO MEFs were prepared from day 13.5 embryos of wild type and $p53^{(+/-)}$ mice [35] as previously described [34] and cultured under the standard 3T3 (Std-3T3) passage protocol [36] or with the following modifications: tSD-3T3. Senescing MEFs (P6 or P8) were maintained under tSD-3T3 conditions for the experiments shown in Figures 2, 3, 4, 5. NHFs (normal human umbilical cord fibroblasts; HUC-F2, RIKEN BRL Cell Bank) were cultured under Std-3T3 conditions. Resveratrol treatment of NHFs was performed as for MEFs. For the H2AX shRNA study, the reported sequence oligonucleotide [37,38] was inserted into the pSuper.retro.puro vector (Oligoengine) and the shRNA virus was then prepared using 293T cells. The virus was infected into NHF cells and selected with puromycin. Mouse tissue samples were prepared from mice at the ages indicated (Sankyo Labo Service).

DNA damage and induction of replication stress

DSB damage was induced by neocarzinostatin (Pola Pharma, Tokyo, Japan) treatment. For induction of DNA replication stress, MEFs were treated with hydroxyurea (HU).

Antibodies, immunostaining and Western blotting

Antibodies against γH2AX (JBW301, Upstate Biotechnology) and H2AX (Bethyl) were used for immunostaining and Western blot analysis. Antibodies against β-actin (AC-74, Sigma), PCNA (Santa Cruz) and histone H3 (ab1791, Abcam) were used for Western blot analysis. Prior to immunostaining with primary and secondary antibodies, cells were fixed with 4% paraformaldehyde for 10 min and permeabilized with 0.1% Triton X-100/PBS for 10 min. Western blot analysis and confocal microscopy were performed as described previously [10].

Transcription level analyses with RT-PCR

Total RNA was extracted from MEFs with the RNeasy system (Sigma). RNA (0.8 μg) was reverse-transcribed using a cDNA Archive kit (Applied Biosystems) and subjected to PCR. The following PCR primers were used: H2axf, 5′-TTGCTTCAGCTTGGTGCTTAG-3′; H2axr, AACTGGTATGAGGCCAGCAAC; β-actinf, CATCCAGGCTGTGCTGTCCCTGTATGC; and β-actinr, GATCTTCATGGTGCTAGGAGCCAGAGC; Trp53-F, CGGATAGTATTTCACCCTCAAGATCCG; Trp53-R, AGCCCTGCTGTCTCCAGACTC; Sidt2-F, CGGAAGGCTGGTTTCTGAGTTTCCG; Sidt2-R, CTGTAAACGCCAAGGACCAGAA; Phlda3-F, CGGTCCATCTAC-

TTCACGCTAGTGACCG; Phlda3-R, TGGATGGCCTGTTGATTCTTGA; Gapdh-F, AACTTTGGCATTGTGGAAGG; Gapdh-R, ATGCAGGGATGATGTTCTGG. The amplified products by Ampli*Taq* Gold (Applied Biosystems) were separated on a 2% agarose gel and visualized with ethidium bromide. Otherwise, real-time PCR assay was carried out using Power SYBER green PCR Master kit (ABI).

Chromosome spreads

Mitotic cells were prepared by treatment with 20 ng/ml nocodazole for 6 h and then collected. The collected cells were swollen hypotonically with 75 mM KCl for 15 min, and then fixed with Carnoy's solution (75% methanol/25% acetic acid) for 20 min. After changing the fixative once, the cells were dropped in Carnoy's solution onto glass slides and air-dried. The slides were stained with 4% Giemsa (Merck) solution for 10 min, washed briefly in tap water, and air-dried.

Supporting Information

Figure S1 Representative images of MEFs during the lifespan. MEFs cultivated as in Figure 1A top lead into either immortality development under Std-3T3 or quiescence preservation under tSD-3T3. After serial cultivation, MEFs become morphologically senescent, i.e., flattened and enlarged morphology (P9) under both Std-3T3 and tSD-3T3 conditions. While continuous MEF-culture under tSD-3T3 preserved the quiescent status with continuously senescent morphology, continuous MEF-culture under Std-3T3 lead to the sporadic emergence of immortalized colony from the senescent MEFs. Immortalized MEFs (IP2) are morphologically escaped from senescence and rather similar to that in early passage (P3).
(TIF)

Figure S2 H2AX diminution is also observed in adult mice organs. Samples were prepared from five week (5W), five month (5M) and seven- or nine-month-old mice (7M or 9M). Compared to five months old organs, H2AX protein level is diminished in Testis (9M), Brain (7M), and Colon (7M), in which the diminution levels are lower than those in Liver, Spleen, and Pancreas. In Heart and Thymus, H2AX levels did not altered the alteration in through 5 weeks old to 7 or 9 months old.
(TIF)

Figure S3 H2AX diminution is also shown in damage induced premature senescence. Premature senescence was induced with NCS treatment as shown schematically in the top, in which each red arrowhead represents 100 ng/μl NCS treatment. Premature senescence by damage was induced with H2AX diminution, in which cells showed typical senescent morphology of flattened and enlarged.
(TIF)

Figure S4 H2AX transcript is decreased in quiescent MEFs. Decrease in H2AX mRNA level in senescing MEFs was observed by RT-PCR (right panel) and is compared with protein diminution (left panel).
(TIF)

Figure S5 H2AX over-expression accelerates immortality development in MEFs with tetraploidy. A. Experimental scheme of H2AX over expression. After transfection of H2AX-over expressing (H2AX-OE) or empty control vectors into early passage MEFs (P3), the transformed MEFs were selected, re-plated, and maintained in complete medium until immortalized cells appeared. **B.** Growth curves of MEFs during the experiments in A. MEFs before transfection and re-plating, MEFs transfected with H2AX-over-expressing vector, and MEFs transfected with empty control vector are indicated by black closed squares, red open circles, and black open diamonds, respectively. MEFs over-expressing H2AX showed accelerated development of immortality. **C.** H2AX status was determined as indicated in the figure. Although senescence was induced in the transfected and selected MEFs, H2AX over-expressing MEFs show higher levels of H2AX after the selection resulting in the development of immortality with H2AX recovery. **D.** Representative MEF images during accelerated immortality development with H2AX over-expression and controls. MEFs transfected with the H2AX over-expressing vector showed an efficient escape from senescence, while MEFs carrying the negative control vectors remained senescent with a flattened and enlarged morphology. **E,F.** Genomic instability status in immortalized MEFs (IP3) that were developed with H2AX over-expression was assessed by flow-cytometry (**E**) and Giemsa staining of M-phase chromosome (**F**).
(TIF)

Figure S6 p53 expression in senescing MEFs. To determine p53 expression in the cause of senescence, the expression levels of p53 and the targets (Sidt2 and Phlda3) that are likely associated with tumor suppression were compared between early passage (P2) and senescent MEFs (P7) under tSD-3T3 conditions. Along with H2AX diminution under p53 proficient background after serial cultivation, the expressions of Sidt2 and Phlda3 were observed in senescent MEFs (P7), in which the change in the expressed p53 transcript is limited.
(TIF)

Figure S7 p53 activation shown by miR34a expression in primary wt-MEFs after damage is not directly associated with H2AX expression levels at least for transcript regulation. A. To confirm p53 dependent DNA damage response, wt- and $p53^{-/-}$-MEFs in primary and immortal were treated with 200 ng/ml neocarzinostatin (NCS) for 6 hours and the expression of p53-target miR34a was assessed. As expected, miR34a expression was shown after NCS treatment in primary wt-MEFs (wild type) but neither in immortalized wt-MEFs nor in $p53^{-/-}$-MEFs. **B.** To determine the p53-activation associated change in the expression levels of H2AX transcript, mRNA levels of H2AX in MEFs treated as in **A** were analyzed. Whereas p53 is activated after NCS treatment in primary wt-MEFs, H2AX transcript levels were stable, suggesting no direct regulation by p53 transcription factor for H2AX expression. The PCR primers for miR34a were used from miRNA-specific primers (ABI) with snoRNA202 (ABI) for the control. Real-time PCR assay was carried out TaqMan microRNA assay kit (ABI).
(TIF)

Acknowledgments

We thank RIKEN BRL Cell Bank for the normal human umbilical cord fibroblast (NHF) cells (HUC-F2). We also thank K. Shimizu-Saito, M. Yanokura, and I. Kobayashi for technical support. We are grateful to S. Takeda, W. Bonner, P. Hsieh, K. Okamoto, and S. Nakada for critical reading of the manuscript and to T. Tsuzuki and Y. Nakatsu for critical discussion of the study.

Author Contributions

Conceived and designed the experiments: KY. Performed the experiments: YA H. Fuji H. Fukuda AI KS YY MS YI JU KY. Analyzed the data: H. Fuji KY. Contributed reagents/materials/analysis tools: SM NT YH HN MM. Wrote the paper: KY H. Fukuda HT.

References

1. Negrini S, Gorgoulis VG, Halazonetis TD (2010) Genomic instability–an evolving hallmark of cancer. Nat Rev Mol Cell Biol 11: 220–228.
2. Lengauer C, Kinzler KW, Vogelstein B (1997) Genetic instabilities in colorectal cancers. Nature 386: 632–627.
3. Lengauer C, Kinzler KW, Vogelstein B (1998) Genetic instabilities in human cancers. Nature 396: 643–649.
4. Stephans PJ, Greenman CD, Fu B, Yang F, Bignell GR, et al. (2011) Massive genomic rearrangement acquired in a single catastrophic event during cancer development. Cell 144: 27–40.
5. Vitale I, Galluzzi L, Senovilla L, Criollo A, Jemaà M, et al. Illicit survival of cancer cells during polyploidization and depolyploidization. Cell death differ, doi: 10.1038/cdd.2010.145.
6. Danes BS (1978) Increased in vitro tetraploidy: tissue specific within the heritable colorectal cancer syndromes with polyposis coli. Cancer 41: 2330–2334.
7. Dutrillaux B, Gerbault-Seureau M, Remvikos Y, Zafrani B, Prieur M (1991) Breast cancer genetic evolution: I. Data from cytogenetics and DNA content. Breast Cancer Res Treat 19: 245–255.
8. Heselmeyer K, Schröck E, du Manoir S, Blegen H, Shah K, et al. (1996) Gain of chromosome 3q defines the transition from severe dysplasia to invasive carcinoma of the uterine cervix. Proc Natl Acad Sci USA 93: 479–484.
9. Maley CC, Galipeau PC, Li X, Sanchez CA, Paulson TG, et al. (2004) The combination of genetic instability and clonal expansion predicts progression to esophageal adenocarcinoma. Cancer Res 64: 7629–7633.
10. Ichijima Y, Yoshioka K, Yoshioka Y, Shinohe K, Fujimori H, et al. (2010) DNA lesions induced by replication stress trigger mitotic aberration and tetraploidy development. PLoS One 5: e8821.
11. Bartkova J, Horejsí Z, Koed K, Krämer A, Tort F, et al. (2005) DNA damage response as a candidate anti-cancer barrier in early human tumorigenesis. Nature 434: 864–870.
12. Gorgoulis VG, Vassiliou LV, Karakaidos P, Zacharatos P, Kotsinas A, et al. (2005) Activation of the DNA damage checkpoint and genomic instability in human precancerous lesions. Nature 434: 907–913.
13. Sedelnikova OA, Horikawa I, Zimonjic DB, Popescu NC, Bonner WM, et al. (2004) Senescing human cells and ageing mice accumulate DNA lesions with unrepairable double-strand breaks. Nature Cell Biol 6: 168–170.
14. Nakamura AJ, Chiang YJ, Hathcock KS, Horikawa I, Sedelnikova OA, et al. (2008) Both telomeric and non-telomeric DNA damage are determinants of mammalian cellular senescence. Epigenetics Chromatin 1: 6.
15. Geigl JB, Langer S, Barwisch S, Pfleghaar K, Lederer G, et al. (2004) Analysis of gene expression patterns and chromosomal changes associated with aging. Cancer Res 64: 8550–8557.
16. Sherr CJ, Weber JD (2000) The ARF/p53 pathway. Curr Opin Genet Dev 10: 94–99.
17. Sherr CJ (1998) Tumor surveillance via the ARF-p53 pathway. Genes Dev 12: 2984–2991.
18. Matheu A, Maraver A, Serrano M (2008) The Arf/p53 pathway in cancer and aging. Cancer Res 68: 6031–6034.
19. Tyner SD, Venkatachalam S, Choi J, Jones S, Ghebranious N, et al. (2002) p53 mutant mice that display early ageing-associated phenotypes. Nature 415: 45–53.
20. Maier B, Gluba W, Bernier B, Turner T, Mohammad K, et al. (2004) Modulation of mammalian life span by the short isoform of p53. Genes Dev 18: 306–319.
21. Varela I, Cadiñanos J, Pendás AM, Gutiérrez-Fernández A, Folgueras AR, et al. (2005) Accelerated ageing in mic deficient in Zmpste24 protease is linked to p53 signalling activation. Nature 437: 564–568.
22. Matheu A, Maraver A, Klatt P, Flores I, Garcia-Cao I, et al. (2007) Delayed ageing through damage protection by the Arf/p53 pathway. Nature 448: 375–379.
23. Parrincello S, Samper E, Krtolica A, Goldstein J, Melov S, et al. (2003) Oxygen sensitivity severely limits the replicative lifespan of murine fibroblasts. Nature Cell Biol 5: 741–746.
24. Bassing CH, Chua KF, Sekiguchi J, Suh H, Whitlow SR, et al. (2002) Increased ionizing radiation sensitivity and genomic instability in the absence of histone H2AX. Proc Natl Acad Sci USA 99: 8173–8178.
25. Celeste A, Petersen S, Romanienko PJ, Fernandez-Capetillo O, Chen HT, et al. (2002) Genomic instability in mice lacking histone H2AX. Science 296: 922–927.
26. Bronson R, Lee C, Alt WF (2003) Histone H2AX: A dosage-dependent suppressor of oncogenic translocations and tumors. Cell 114: 359–370.
27. Bassing CH, Alt FW (2004) H2AX May Function as an Anchor to Hold Broken Chromosomal DNA Ends in Close Proximity. Cell Cycle 3: 149–153.
28. Bonner WM, Redon CE, Dickey JS, Nakamura AJ, Sedelnikova OA, et al. (2008) GammaH2AX and cancer. Nature Rev Cancer 8: 957–967.
29. Tsukuda T, Fleming AB, Nickoloff JA, Osley MA (2005) Chromatin remodelling at a DNA double-strand break site in Saccharomyces cerevisiae. Nature 438: 379–383.
30. Keogh MC, Mennella TA, Sawa C, Berthelet S, Krogan NJ, et al. (2006) The Saccharomyces cerevisiae histone H2A variant Htz1 is acetylated by NuA4. Genes Dev 20: 660–665.
31. Ikura T, Tashiro S, Kakino A, Shima H, Jacob N, et al. (2007) DNA damage-dependent acetylation and ubiquitination of H2AX enhances chromatin dynamics. Mol Cell Biol 27: 7028–7040.
32. Brady CA, Jiang D, Mello SS, Johnson TM, Jarvis LA, et al. (2011) Distinct p53 transcriptional programs dictate acute DNA-damage responses and tumor suppression. Cell 145: 571–583.
33. Ceribelli M, Alcalay M, Viganò MA, Mantovani R (2006) Repression of new p53 targets revealed by ChIP on chip experiments. Cell Cycle 5: 1102–1110.
34. Yoshioka K, Yoshioka Y, Hsieh P (2006) ATR kinase activation mediated by MutSα and MutLα in response to cytotoxic O6-methylguanine adducts. Mol Cell 22: 501–510.
35. Tatemichi M, Tazawa H, Masuda M, Saleem M, Wada S, et al. (2004) Suppression of thymic lymphomas and increased nonthymic lymphomagenesis in Trp53-deficient mice lacking inducible nitric oxide synthase gene. Int J Cancer 111: 819–828.
36. Todaro GJ, Green H (1963) Quantitative studies of the growth of mouse embryo cells in culture and their development into established lines. J Cell Biol 17: 299–313.
37. Lukas C, Melander F, Stucki M, Falck J, Bekker-Jensen S, et al. (2004) Mdc1 couples DNA double-strand break recognition by Nbs1 with its H2AX-dependent chromatin retention. EMBO J 23: 2674–2683.
38. Dimitrova N, de Lange T (2006) MDC1 accelerates nonhomologous end-joining of dysfunctional telomeres. Genes Dev 20: 3238–3243.

blood

2011 117: 2887-2890
Prepublished online November 9, 2010;
doi:10.1182/blood-2010-08-301515

Autoimmune lymphoproliferative syndrome–like disease with somatic *KRAS* mutation

Masatoshi Takagi, Kunihiro Shinoda, Jinhua Piao, Noriko Mitsuiki, Mari Takagi, Kazuyuki Matsuda, Hideki Muramatsu, Sayoko Doisaki, Masayuki Nagasawa, Tomohiro Morio, Yoshihito Kasahara, Kenichi Koike, Seiji Kojima, Akira Takao and Shuki Mizutani

Blood (print ISSN 0006-4971, online ISSN 1528-0020), is published weekly by the American Society of Hematology, 2021 L St, NW, Suite 900, Washington DC 20036.

Brief report

Autoimmune lymphoproliferative syndrome–like disease with somatic *KRAS* mutation

Masatoshi Takagi,[1] Kunihiro Shinoda,[2] Jinhua Piao,[1] Noriko Mitsuiki,[1] Mari Takagi,[2] Kazuyuki Matsuda,[3] Hideki Muramatsu,[4] Sayoko Doisaki,[4] Masayuki Nagasawa,[1] Tomohiro Morio,[1] Yoshihito Kasahara,[5] Kenichi Koike,[6] Seiji Kojima,[4] Akira Takao,[2] and Shuki Mizutani[1]

[1]Department of Pediatrics and Developmental Biology, Graduate School of Medicine, Tokyo Medical and Dental University, Tokyo, Japan; [2]Department of Pediatrics, Gifu Municipal Hospital, Gifu, Japan; [3]Department of Laboratory Medicine, Shinshu University School of Medicine, Nagano, Japan; [4]Department of Pediatrics, Nagoya University Graduate School of Medicine, Aichi, Japan; [5]Department of Laboratory Sciences, Kanazawa University School of Health Sciences, Ishikawa, Japan; and [6]Department of Pediatrics, Shinshu University School of Medicine, Nagano, Japan

Autoimmune lymphoproliferative syndrome (ALPS) is classically defined as a disease with defective FAS-mediated apoptosis (type I-III). Germline *NRAS* mutation was recently identified in type IV ALPS. We report 2 cases with ALPS-like disease with somatic *KRAS* mutation. Both cases were characterized by prominent autoimmune cytopenia and lymphoadenopathy/splenomegaly. These patients did not satisfy the diagnostic criteria for ALPS or juvenile myelomonocytic leukemia and are probably defined as a new disease entity of RAS-associated ALPS-like disease (RALD). (*Blood.* 2011;117(10):2887-2890)

Introduction

Autoimmune lymphoproliferative syndrome (ALPS) is a disease characterized by dysfunction of the FAS-mediated apoptotic pathway,[1,2] currently categorized as: type Ia, germline *TNFRSF6/FAS* mutation; type Ib, germline *FAS ligand* mutation; type Is, somatic *TNFRSF6/FAS* mutation; and type II, germline *Caspase 10* mutation. Patients exhibit lymphadenopathy, hepatosplenomegaly, and autoimmune diseases, such as immune cytopenia and hyper-γ-globulinemia. An additional subclassification has been proposed that includes types III and IV, whereby type III has been defined as that with no known mutation but with a defect in FAS-mediated apoptosis and type IV as one showing germline *NRAS* mutation.[3] Type IV is considered exceptional because the FAS-dependent apoptosis pathway is not involved in the pathogenesis, and this subclass is characterized by a resistance to interleukin-2 (IL-2) depletion-dependent apoptosis. Recent updated criteria and classification of ALPS suggested type IV ALPS as a RAS-associated leukoproliferative disease.[4]

Juvenile myelomonocytic leukemia (JMML) is a chronic leukemia in children. Patients show lymphadenopathy, hepatosplenomegaly, leukocytosis associated with monocytosis, anemia, thrombocytopenia, and occasional autoimmune phenotypes. Approximately 80% of patients with JMML have been shown to have a genetic abnormality in their leukemia cells, including mutations of *NF1*, *RAS* family,[5] *CBL*, or *PTPN11*. The hallmarks of the laboratory findings of JMML include spontaneous colony formation in bone marrow (BM) or peripheral blood mononuclear cells (MNCs) and hypersensitivity to granulocyte-macrophage colony-stimulating factor (GM-CSF) of $CD34^+$ BM-MNCs.[6]

Germline RAS pathway mutations cause Costello (*HRAS*), Noonan (*PTPN11*, *KRAS*, and *SOS1*), and cardio-facio-cutaneous syndromes (*KRAS*, *BRAF*, *MEK1*, and *MEK2*). Patients with Costello and Noonan syndromes have an increased propensity to develop solid and hematopoietic tumors, respectively[7]; among these tumors, the incidence of JMML in patients with germline mutation of *NF1* or *PTPN11* is well known.

We present 2 cases with autoimmune cytopenia and remarkable lymphadenopathy and hepatosplenomegaly, both of which were identified as having a somatic KRAS G13D mutation without any clinical features of germline *RAS* mutation, such as cardio-facio-cutaneous or Noonan syndrome.

Methods

All studies were approved by the ethical board of Tokyo Medical and Dental University.

Case 1

A 9-month-old boy had enormous bilateral cervical lymphadenopathy and hepatosplenomegaly (supplemental Figure 1A-B, available on the *Blood* Web site; see the Supplemental Materials link at the top of the online article). Blood test revealed the presence of hemolytic anemia and autoimmune thrombocytopenia. Hyper-γ-globulinemia with various autoantibodies was also noted. ALPS and JMML were nominated as the diseases to be differentially diagnosed. Detailed clinical history and laboratory data are provided as Supplemental data. The patient did not satisfy the criteria for the diagnosis of ALPS or JMML as discussed in "Results and discussion."

Submitted August 10, 2010; accepted October 27, 2010. Prepublished online as *Blood* First Edition paper, November 9, 2010; DOI 10.1182/blood-2010-08-301515.

An Inside *Blood* analysis of this article appears at the front of this issue.

The online version of this article contains a data supplement.

The publication costs of this article were defrayed in part by page charge payment. Therefore, and solely to indicate this fact, this article is hereby marked "advertisement" in accordance with 18 USC section 1734.

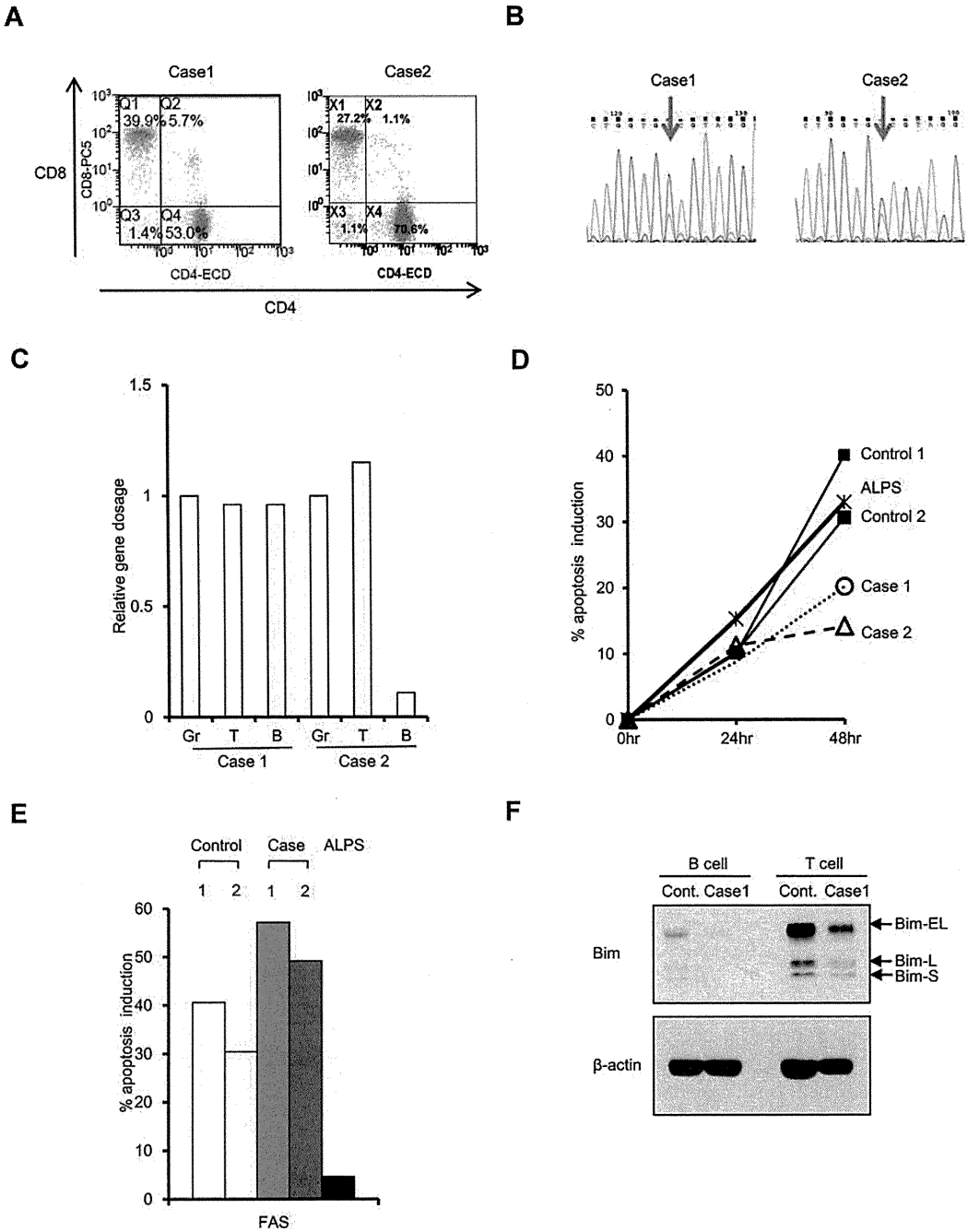

Figure 1. Molecular cell biologic assay of RALD. (A) Flow cytometric analysis of double-negative T cells. CD8 and CD4 double staining was performed in T-cell receptor-αβ-expressing cells. (B) Electropherogram showing KRAS G13D mutation in BM-MNCs in case 1 (left panel) and case 2 (right panel). (C) Gene dosage of mutated allele in granulocytes (Gr), T cells (T), and B cells (B). Relative gene dosage was estimated by a mutant allele-specific polymerase chain reaction method in cases 1 and 2 using albumin gene as internal control. (D) Apoptosis assay using activated T cells. Apoptosis percentage was measured by flow cytometry with annexin V staining 24 and 48 hours after IL-2 depletion. (E) Apoptosis percentage was measured 24 hours after addition of anti-FAS CH11 antibody (final 100 ng/mL). (F) Western blotting analysis of Bim expression.

Case 2

A 5-month-old girl had a fever and massive hepatosplenomegaly (supplemental Figure 1D). She was initially diagnosed with Evans syndrome based on the presence of hemolytic anemia and autoimmune thrombocytopenia with hyper-γ-globulinemia and autoantibodies. Spontaneous colony formation assay and GM-CSF hypersensitivity of BM-MNCs showed positivity. Then, tentative diagnosis of JMML was given, even though she showed no massive monocytosis or increased fetal hemoglobin. Detailed clinical history and laboratory data are provided in supplemental data.

Detailed methods for experiments are described in supplemental data.

Results and discussion

Case 1 showed a high likelihood of being a case of ALPS according to the symptoms and clinical data presented (supplemental Table 1), except for number of double-negative T cells, which was only 1.4% of T-cell receptor-αβ cells (Figure 1A). JMML was also nominated as a disease to be differentiated because remarkable hepatosplenomegaly with thrombocythemia and moderate monocytosis was

noted. However, no hypersensitivity to GM-CSF as determined by colony formation assay for BM-MNCs (data not shown) or phosphor-STAT5 staining (data not shown) was observed. DNA sequence for JMML-associated genes, such as *NRAS, KRAS, HRAS, PTPN11*, and *CBL*, was determined, and KRAS G13D mutation was identified (Figure 1B). The mutation was seen exclusively in the hematopoietic cell lineage, and no mutation was seen in the oral mucosa or nail-derived DNA. Granulocytes, monocytes, T cells, and B cells were all positive for KRAS G13D mutation (data not shown). The proportion of mutated cells in each hematopoietic lineage was quantitated by mutation allele-specific quantitative polymerase chain reaction methods, which revealed that mutated allele was almost equally present in granulocytes, T cells, and B cells (Figure 1C). $CD34^+$ hematopoietic stem cells (HSCs) were also positive for KRAS G13D mutation, and 60% of colony-forming units-granulocyte macrophage (CFU-GM) developed from isolated CD34 cells carried the KRAS G13D mutation (data not shown). These observations suggest that the mutation occurred at the HSCs level, and HSC consists of wild-type and mutant HSCs.

NRAS-mutated type IV ALPS was previously characterized by apoptosis resistance of T cells in IL-2 depletion.[3] Then, activated T cells were subjected to an apoptosis assay by FAS stimulation or IL-2 depletion. Remarkable resistance to IL-2 depletion, but not to FAS-dependent apoptosis (Figure 1D-E), was seen. This was in contrast to T cells from FAS-mutated ALPS type 1a, which showed remarkable resistance to FAS-dependent apoptosis and normal apoptosis induction by IL-2 withdrawal (Figure 1D-E). Western blotting analysis of activated T cells or Epstein-Barr virus-transformed B cells showed reduced expression of Bim (Figure 1F).

In case 2, autoimmune phenotype and hepatosplenomegaly were remarkable, as shown in Supplemental data. The patient was initially diagnosed as Evans syndrome based on the presence of hemolytic anemia and autoimmune thrombocytopenia. Double-negative T cells were 1.1% of T-cell receptor-$\alpha\beta$ cells in the peripheral blood, which did not meet with the criteria of ALPS. Although spontaneous colony formation was shown in peripheral blood- and BM-MNCs, and GM-CSF hypersensitivity was demonstrated in BM-MNCs derived $CD34^+$ cell (supplemental Table 2), she showed no massive monocytosis or increased fetal hemoglobin. Thus, the diagnosis was less likely to be ALPS or JMML. DNA sequencing of JMML-related genes, such as *NRAS, KRAS, HRAS, PTPN11*, and *CBL*, identified somatic, but not germline, KRAS G13D mutation (Figure 1B). KRAS G13D mutation was detected in granulocytes and T cells. Mutation was not identified in B cells by conventional DNA sequencing (data not shown). Mutant allele-specific quantitative polymerase chain reaction revealed that mutated allele was almost equally present in granulocytes and T cells, but barely in B cells (Figure 1C). Activated T cells showed resistance to IL-2 depletion but not to FAS-dependent apoptosis (Figure 1D-E).

Both of our cases were characterized by strong autoimmunity, immune cytopenia, and lymphadenopathy or hepatosplenomegaly with partial similarity with ALPS or JMML. However, they did not meet with the well-defined diagnostic criteria of ALPS[2] or JMML.[6] It is interesting that case 2 presented GM-CSF hypersensitivity, which is one of the hallmarks of JMML. Given the strict clinical and laboratory criteria of JMML and ALPS, our 2 cases should be defined as a new disease entity, such as RAS-associated ALPS-like disease (RALD). Recently defined NRAS-mutated ALPS type IV may also be included in a similar disease entity.

There are several cases of JMML reported simultaneously having clinical and laboratory findings compatible with autoimmune disease.[8,9] Autoimmune syndromes are occasionally seen in patients with myelodysplastic syndromes, including chronic myelomonocytic leukemia.[10] These previous findings may suggest a close relationship of autoimmune disease and JMML. Because KRAS G13D has been identified in JMML,[11-13] it is tempting to speculate that KRAS G13D mutation is involved in JMML as well as RALD. In JMML, erythroid cells reportedly carry mutant RAS, whereas B- and T-cell involvement was variable.[13] In both of our cases, myeloid cells and T cells carried mutant RAS, whereas B cells were affected variably. These findings would support a hypothesis that the clinical and hematologic features are related to the differentiation stages of HSCs where RAS mutation is acquired. JMML-like myelomonocytic proliferation may predict an involvement of RAS mutation in myeloid stem/precursor cell level, whereas ALPS-like phenotype may predict that of stem/precursor cells of lymphoid lineage, especially of T cells. Under the light of subtle differences between the 2 cases presented, their hematologic and clinical features may reflect the characteristics of the stem cell level where *KRAS* mutation is acquired. Involvement of the precursors with higher propensity toward lymphoid lineage may lead to autoimmune phenotypes, whereas involvement of those with propensity toward the myeloid lineage may lead to GM-CSF hypersensitivity while still sharing some overlapping autoimmune characteristics.

One may argue from the other viewpoints with regard to the clinicopathologic features of these disorders. First, transformation in fetal HSCs might be obligatory for the development of JMML[14] and, in HSCs later in life, may not have the same consequences. Second, certain KRAS mutations may be more potent than others. Codon 13 mutations are generally less deleterious biochemically than codon 12 substitutions, and patients with JMML with codon 13 mutations have been reported to show spontaneous hematologic improvement.[12,15] Thus, further studies are needed to reveal in-depth clinicopathologic characteristics in this type of lymphomyeloproliferative disorder.

KRAS mutation may initiate the oncogenic pathway as one of the first genetic hits but is insufficient to cause frank malignancy by itself.[16,17] Considering recent findings that additional mutations of the genes involved in DNA repair, cell cycle arrest, and apoptosis are required for full malignant transformation, one can argue that RALD patients will also develop malignancies during the course of the disease. Occasional association of myeloid blast crisis in JMML and that of lymphoid malignancies in ALPS will support this notion. Thus, the 2 patients are now being followed up carefully. It was recently revealed that half of the patients diagnosed with Evans syndrome, an autoimmune disease presenting with hemolytic anemia and thrombocytopenia, met the criteria for ALPS diagnosis.[18,19] In this study, FAS-mediated apoptosis analysis was used for the screening. Considering the cases we presented, it will be intriguing to reevaluate Evans syndrome by IL-2 depletion-dependent apoptosis assay focusing on the overlapping autoimmunity with RALD.

Acknowledgments

This work was supported by the Ministry of Education, Science, and Culture of Japan (Grant-in-Aid 20390302; S.M.) and the

Ministry of Health, Labor and Welfare of Japan (Grant-in-Aid for Cancer Research 20-4 and 19-9; S.M., Masatoshi Takagi).

Authorship

Contribution: Masatoshi Takagi and S.M. designed entire experiments and wrote the manuscript; K.S., N.M., and Mari Takagi treated patients and designed clinical laboratory test; J.P. performed experiments described in Figure 1B-F; K.M., H.M., and S.D. performed colony and mutational analysis; and M.N., T.M., K.K., S.K., Y.K., and A.T. supervised clinical and immunologic experiments or coordinated clinical information.

Conflict-of-interest disclosure: The authors declare no competing financial interests.

Correspondence: Masatoshi Takagi, Department of Pediatrics and Developmental Biology, Graduate School of Medicine, Tokyo Medical and Dental University, 1-5-45 Yushima, Bunkyo-ku, Tokyo, 113-8519, Japan; e-mail: m.takagi.ped@tmd.ac.jp; and Shuki Mizutani, Department of Pediatrics and Developmental Biology, Graduate School of Medicine, Tokyo Medical and Dental University, 1-5-45 Yushima, Bunkyo-ku, Tokyo, 113-8519, Japan; e-mail: smizutani.ped@tmd.ac.jp.

References

1. Fisher GH, Rosenberg FJ, Straus SE, et al. Dominant interfering Fas gene mutations impair apoptosis in a human autoimmune lymphoproliferative syndrome. *Cell.* 1995;81(6):935-946.
2. Teachey DT, Seif AE, Grupp SA. Advances in the management and understanding of autoimmune lymphoproliferative syndrome (ALPS). *Br J Haematol.* 2010;148(2):205-216.
3. Oliveira JB, Bidere N, Niemela JE, et al. NRAS mutation causes a human autoimmune lymphoproliferative syndrome. *Proc Natl Acad Sci U S A.* 2007;104(21):8953-8958.
4. Oliveira J, Bleesing J, Dianzani U, et al. Revised diagnostic criteria and classification for the autoimmune lymphoproliferative syndrome (ALPS): report from the 2009 NIH International Workshop. *Blood.* 2010;116(14):e35-e40.
5. Miyauchi J, Asada M, Sasaki M, Tsunematsu Y, Kojima S, Mizutani S. Mutations of the N-ras gene in juvenile chronic myelogenous leukemia. *Blood.* 1994;83(8):2248-2254.
6. Emanuel PD. Juvenile myelomonocytic leukemia and chronic myelomonocytic leukemia. *Leukemia.* 2008;22(7):1335-1342.
7. Aoki Y, Niihori T, Narumi Y, Kure S, Matsubara Y. The RAS/MAPK syndromes: novel roles of the RAS pathway in human genetic disorders. *Hum Mutat.* 2008;29(8):992-1006.
8. Kitahara M, Koike K, Kurokawa Y, et al. Lupus nephritis in juvenile myelomonocytic leukemia. *Clin Nephrol.* 1999;51(5):314-318.
9. Oliver JW, Farnsworth B, Tonk VS. Juvenile myelomonocytic leukemia in a child with Crohn disease. *Cancer Genet Cytogenet.* 2006;167(1):70-73.
10. Saif MW, Hopkins JL, Gore SD. Autoimmune phenomena in patients with myelodysplastic syndromes and chronic myelomonocytic leukemia. *Leuk Lymphoma.* 2002;43(11):2083-2092.
11. Flotho C, Kratz CP, Bergstrasser E, et al. Genotype-phenotype correlation in cases of juvenile myelomonocytic leukemia with clonal RAS mutations. *Blood.* 2008;111(2):966-967.
12. Matsuda K, Shimada A, Yoshida N, et al. Spontaneous improvement of hematologic abnormalities in patients having juvenile myelomonocytic leukemia with specific RAS mutations. *Blood.* 2007; 109(12):5477-5480.
13. Flotho C, Valcamonica S, Mach-Pascual S, et al. RAS mutations and clonality analysis in children with juvenile myelomonocytic leukemia (JMML). *Leukemia.* 1999;13(1):32-37.
14. Matsuda K, Sakashita K, Taira C, et al. Quantitative assessment of PTPN11 or RAS mutations at the neonatal period and during the clinical course in patients with juvenile myelomonocytic leukaemia. *Br J Haematol.* 2010;148(4):593-599.
15. Imamura M, Imai C, Takachi T, Nemoto T, Tanaka A, Uchiyama M. Juvenile myelomonocytic leukemia with less aggressive clinical course and KRAS mutation. *Pediatr Blood Cancer.* 2008;51(4):569.
16. Zhang J, Wang J, Liu Y, et al. Oncogenic Kras-induced leukemogeneis: hematopoietic stem cells as the initial target and lineage-specific progenitors as the potential targets for final leukemic transformation. *Blood.* 2009;113(6):1304-1314.
17. Sabnis AJ, Cheung LS, Dail M, et al. Oncogenic Kras initiates leukemia in hematopoietic stem cells. *PLoS Biol.* 2009;7(3):0537-0548.
18. Teachey DT, Manno CS, Axsom KM, et al. Unmasking Evans syndrome: T-cell phenotype and apoptotic response reveal autoimmune lymphoproliferative syndrome (ALPS). *Blood.* 2005; 105(6):2443-2448.
19. Seif AE, Manno CS, Sheen C, Grupp SA, Teachey DT. Identifying autoimmune lymphoproliferative syndrome in children with Evans syndrome: a multi-institutional study. *Blood.* 2010; 115(11):2142-2145.